An alternative surplus production model

Peter Sheldon Rankin[*], Ricardo T. Lemos[†‡]

June 18, 2015

Abstract

In this work we present a novel surplus production model for fisheries stock assessment. Our goal is to enhance parameter estimation and fitting speed. The model employs a production function that differs from the canonical logistic (Schaefer) and Gompertz (Fox) functions, but is still connected to the Pella-Tomlinson formulation. We embed this function in a state-space model, using observed catch-per-unit-effort indices and measures of fishing effort as input. From the literature we derive Bayesian prior densities for all model hyperparameters (carrying capacity, catchability, growth rate and error variance), as well as the state (annual stock biomass). We use the

[*]Corresponding author: ARC Centre of Excellence for Environmental Decisions, School of Biological Sciences, The University of Queensland, St. Lucia 4072, Queensland, Australia. Email: p.rankin@uqconnect.edu.au Phone: +61 403 885 724.

[†]Centre for Applications in Natural Resource Mathematics, School of Mathematics and Physics, The University of Queensland, St. Lucia 4072, Queensland, Australia.

[‡]The Climate Corporation, 201 3rd St., suite 1100, San Francisco, California 94103, USA. Email: ricardo.lemos@climate.com

well-studied Namibian hake fishery as a case study, via which we compare the Schaefer, Fox and Pella-Tomlinson models with the new model. We also develop a package for the software `R`, which employs a Shiny application for data exploration, model specification, and output analyses. Posterior densities of hyperparameters and reference points agree across models. Identifiability issues emerge in the more cumbersome Pella-Tomlinson model. The new model yields small but consistent improvements in precision. It also renders implementation faster and easier, with no hidden truncation of negative biomasses. We conclude by discussing theoretical and practical extensions to this new model.

Keywords

Surplus production model; stock assessment; Bayesian inference; fisheries models; management reference points

1 Introduction

Surplus production models provide simple descriptions of harvested populations, in terms of annual biomass levels (B_t), the intrinsic growth rate (r), the carrying capacity of the environment (K) and the efficiency of fishing gear (q; Hilborn and Walters, 1992; Polacheck et al., 1993). The basic concepts underlying these models were introduced by Graham (1935) and developed by Schaefer (1954), Beverton and Holt (1957), Pella and Tomlinson (1969) and Fox (1970). Albeit criticized for their potentially excessive simplicity (Megrey and Wespestad, 2013; Wang et al., 2014), surplus production models are still widely used today,

to generate reference points for fisheries management, such as maximum sustainable yield (Hilborn, 2001; Zhang, 2013).

Several approaches have been employed to estimate parameters in surplus production models. Examples include ordinary least squares (Uhler, 1980), maximum likelihood (Gould and Pollock, 1997) and Bayesian inference (Walters and Ludwig, 1994). Some methods entail important assumptions, such as equilibrium, the existence of process and/or observation error, and prior information (Hilborn and Walters, 1992; Polacheck et al., 1993; Kuparinen et al., 2012).

Despite the parsimonious parameterisation of surplus production models, inference can be problematic. Often, the only information available stems from catch and effort data, which may not suffice for reliable inference (Hilborn and Walters, 1992; Xiao, 1998; Quinn and Deriso, 1999; Chen, 2003; Magnusson and Hilborn, 2007; Conn et al., 2010; Glaser et al., 2011; Cook, 2013). In light of this, it is important to examine posterior parameter correlation structure and uncertainty (Parent and Rivot, 2012), to avoid erroneous model output interpretation and mismanagement (Ludwig and Walters, 1981; Schnute and Richards, 2001; Needle, 2002; Wang et al., 2009; Conn et al., 2010; He et al., 2011).

When full estimation appears unfeasible, setting some model parameters to assumed fixed values is common in fisheries stock assessment modelling. However, several authors have found this to be poor practice (Rose and Cowan, 2003; Brooks et al., 2010; Brodziak and Ishimura, 2011; Lee et al., 2012). For instance, Mangel et al. (2013) showed that holding steepness and natural mortality constant fully determined key management reference points,

whilst Gould et al. (1997) observed that ignoring variability in catch and effort data could overestimate the size of a fish stock by 20%.

Given the difficulties in estimation and the advice against setting too many constants, new estimation and modelling methods are still sought (Kuparinen et al., 2012). In this work, we propose a new surplus production model that facilitates parameter estimation. We establish a connection between the classical formulation Pella and Tomlinson (1969) and ours. After manipulation, we obtain a hierarchical multiplicative model, which can be linearised with respect to most parameters, via logarithmic transformation. To conduct Bayesian inference, we set up priors for all parameters. We describe how the model can be fitted to the well-studied Namibian hake fishery data set, and demonstrate benefits of the new model by comparing results with the Schaefer, Fox and Pella-Tomlinson surplus production models (Hilborn and Mangel, 1997; McAllister and Kirkwood, 1998; Parent and Rivot, 2012).

2 Methods

2.1 Data

We use catch (thousands of tons) and effort (thousands of hours trawled) data from the Namibian hake (*Merlucius capensis* and *M. paradoxus*) fishery, ICSEAF divisions 1.3 and 1.4, for the years 1965 to 1988 (ICSEAF, 1986; McAllister and Kirkwood, 1998). This fishery consisted of Spanish bottom trawlers in tonnage class 7 (1000-1999 GRT; Andrew, 1986).

2.2 Model

Bayesian state-space models typically consist of three layers (Berliner, 1996). The process layer characterises the temporal dynamics of a stochastic process, as a function of (time-invariant) hyperparameters. An observation layer connects this process with the observable variables. The third layer contains a description of the (prior) probability distribution of the hyperparameters and the state at the first time instant. In the sections below, we specify these three components, in the context of a surplus production model.

2.2.1 Standard process layer

In most situations, the total biomass (B) of an exploited population cannot be observed directly. Nevertheless, we may postulate a standard equation for its dynamics in discrete time t (Parent and Rivot, 2012), as

$$B_{t+1} = B_t + h(B_t) - C_t. \tag{1}$$

In this equation, C_t denotes total catch and $h(B_t)$ is a production function, that is, a parametric function that provides an estimate of biomass growth given its current level (Hilborn and Walters, 1992). In the classical approach of Pella and Tomlinson (1969), $h(B_t)$ is defined as

$$h(B_t) = \frac{r}{\phi} B_t \left(1 - \left(\frac{B_t}{K}\right)^{\phi}\right), \tag{2}$$

where r is the intrinsic rate of population growth, K is the carrying capacity of the environ-

ment and ϕ is a shape parameter. This leads to the production model

$$B_{t+1} = \left(1 + \frac{r}{\phi}\left(1 - \frac{B_t}{K}\right)^{\phi}\right) B_t - C_t. \tag{3}$$

With $\phi = 1$, the Schaefer (1954) production model is obtained:

$$B_{t+1} = \left(1 + r\left(1 - \frac{B_t}{K}\right)\right) B_t - C_t. \tag{4}$$

At the other extreme, the limit $\phi \to 0$ yields the Fox production model (Fox, 1970):

$$B_{t+1} = \left(1 + r\left(1 - \frac{\log B_t}{\log K}\right)\right) B_t - C_t. \tag{5}$$

From a theoretical standpoint, the addition of ϕ to the set of unknowns is sensible, as it allows the surplus production curve to be asymmetric in relation to stock size (Hilborn and Walters, 1992). However, many authors recommend fixing it, as fisheries data tend to be uninformative (Fletcher, 1978; Rivard and Bledsoe, 1978; Hilborn and Walters, 1992; Zhang, 2013).

The three process models described above can become stochastic, by multiplying the right hand side of the equations with $\exp[\epsilon_t]$, such that $\epsilon_t \sim N[0, \sigma]$, i.e. ϵ_t is i.i.d. Normal with mean zero and variance σ (Parent and Rivot, 2012).

2.2.2 Alternative process layer

While the Schaefer and Fox simplifications fix ϕ and keep r free, in this work we explore the opposite approach, which leads us to a more tractable equation for biomass dynamics. Specifically, we let the stock's intrinsic growth rate be a function of depletion ratio and shape

parameter ϕ,

$$r_t = \phi \left(\frac{B_t}{K} \right)^{-\phi}, \tag{6}$$

yielding the production function

$$h(B_t) = \frac{r_t}{\phi} B_t \left(1 - \left(\frac{B_t}{K} \right)^{\phi} \right). \tag{7}$$

Hence, our approach also relinquishes one parameter (r) from the three available in the Pella-Tomlinson model; ϕ, on the other hand, is free but restricted to the interval (0,1).

Next, we point out that total catch, C, is often only partly observable, since it includes reported and unreported catches, as well as discards. Therefore, instead of C, we employ the fishing mortality rate F (also unobservable), such that

$$C_t = \left(1 - e^{-F_t}\right) \times (B_t + h(B_t)) \tag{8}$$

and

$$F_t \sim N[qE_t, \sigma]. \tag{9}$$

In eq. (9), q is the (time-invariant and unknown) catchability parameter, and E is the (measurable) fishing effort. Randomness, with variance σ, may derive from transient fluctuations and possible long-term trends, unaccounted for fishing effort.

With eqs. (6), (7) and (8), eq. (1) simplifies to a product (Appendix A1):

$$B_{t+1} = B_t^{1-\phi} K^{\phi} e^{-F_t}. \tag{10}$$

In equation (10), the consequences of extreme values of ϕ are worth studying. If $\phi = 1$, then biomass always bounces back to the carrying capacity, before the stock is harvested.

In contrast, $\phi = 0$ leads inexorably to extinction, even for mild fishing mortalities. Based on these results, we call ϕ an elasticity parameter, and dub populations with high/low values of ϕ elastic/inelastic (see Appendix A.3 for illustration).

2.2.3 Reparameterization

To prepare the model for log-transformation, we reparameterize a few quantities in the process equation (10): define $\rho = \log(K)$ as the log-carrying capacity; let $\chi = \log(q)$ represent the log-catchability parameter; write $\beta_t = \log(B_t/K)$ as the log-transformed scaled biomass; and define the error term $\epsilon_t \sim N[0, \sigma]$.

With this new set of parameters, eq. (10) may be written as (Appendix A.2)

$$\beta_{t+1} = (1 - \phi)\beta_t - e^{\chi} E_t + \epsilon_t. \tag{11}$$

2.2.4 Observation layer

Fisheries data generally consist of commercial catch and effort records, from which Catch Per Unit Effort (CPUE) indices may be constructed (i_t, $t = 1, \ldots, n$). The latter are assumed proportional to current biomass, that is, $i_t = qB_t$, with q being a constant catchability over time. In other words, the value of q defines how many fish are caught (in the appropriate units), on average, for each unit of fishing effort. Parent and Rivot (2012), among others, build upon this structure by inserting log-normally distributed errors, to reach the stochastic observation equation

$$i_t = qB_t e^{\omega_t}, \tag{12}$$

where $\omega_t \sim N[0, \sigma]$. Note that the variance of ω_t, σ, matches that of ϵ_t. Although such equivalence is not required in state-space models, we use it in order to compare our results to those of Parent and Rivot (2012), as detailed below.

With $Y_t = \log(i_t)$ denoting the observed log-CPUE index, and using the set of parameters described in the process layer, equation (12) can also be written as (Appendix B)

$$Y_t = \chi + \beta_t + \rho + \omega_t. \tag{13}$$

It is worth noting that, in their final form, both the alternative process equation (11) and the observation equation (13) are linear with respect to most parameters. To our knowledge, this result cannot be obtained in Schaefer, Fox, or other variants of Pella-Tomlinson surplus production models.

2.2.5 Hyperparameter layer

In summary, we have presented four surplus production models to estimate annual biomass, catchability, carrying capacity, and either intrinsic growth rate or elasticity. The standard Pella-Tomlinson, Schaefer and Fox models comprise process equations (3), (4), and (5), respectively, together with observation equation (12). The alternative model uses equations (11) and (13) instead. In both models, the random shocks associated with these equations are $\epsilon_t \sim N[0, \sigma]$ and $\omega_t \sim N[0, \sigma]$, respectively. The hyperparameters for Schaefer and Fox models are K, q, r and σ; the Pella-Tomlinson model also has ϕ; the alternative model has ρ, χ, ϕ and σ.

We follow the approach of Parent and Rivot (2012) and employ broad, independent and

uniform prior distributions for all hyperparameters, or transformations thereof (Table 1). To render unrealistic fishing mortality rates less likely, we use tighter prior bounds for χ.

In state-space models, the probability distribution of the state at $t = 1$ is often specified with fixed mean and variance, to avoid increasing the number of unknowns in the model. In surplus production models, Parent and Rivot (2012) suggest centering initial biomass (B_1) at the carrying capacity (K) whenever fishing pressure is absent before the start of the time series. Given this, we let $B_1 \sim LogNormal[K, \sigma]$, or equivalently, $\beta_1 \sim N[0, \sigma]$.

2.3 Reference points

Surplus production models provide useful fishing reference points for management (Punt and Szuwalski, 2012). Here we present three quantities of interest, associated with Maximum Sustainable Yield (MSY), for the four models.

Expressions from Parent and Rivot (2012) for reference points under the Schaefer model are provided first. As the logistic production function is symmetric, the biomass that sustains the maximum sustainable yield is half the carrying capacity,

$$B_{\text{MSY}} = \frac{K}{2}. \tag{14}$$

MSY is then a proportion of the product of population growth and carrying capacity,

$$\text{MSY} = \frac{r \times K}{4}, \tag{15}$$

whilst F_{MSY} is the proportion of biomass removed from B_{MSY} that equals MSY,

$$F_{\text{MSY}} = \frac{\text{MSY}}{B_{\text{MSY}}}. \tag{16}$$

Reference points for the Fox model are similar:

$$B_{\mathrm{MSY}} = \frac{K}{\exp(1)}, \tag{17}$$

$$\mathrm{MSY} = \frac{r \times K}{\exp(1) \times \log K}, \tag{18}$$

$$F_{\mathrm{MSY}} = \frac{\mathrm{MSY}}{B_{\mathrm{MSY}}}. \tag{19}$$

For the Pella-Tomlinson model, reference points depend also on the elasticity parameter ϕ:

$$B_{\mathrm{MSY}} = K \times (1+\phi)^{-\frac{1}{\phi}}, \tag{20}$$

$$\mathrm{MSY} = r \times K \times (1+\phi)^{-\frac{1+\phi}{\phi}}, \tag{21}$$

$$F_{\mathrm{MSY}} = \frac{r}{\phi + 1}. \tag{22}$$

For the alternative model, the level of biomass that maximises yield (B_{MSY}) is found by taking the derivative of the production function (7) with respect to biomass, equating the result to zero and solving the equation analytically:

$$B_{\mathrm{MSY}} = (1-\phi)^{\frac{1}{\phi}} e^{\rho}. \tag{23}$$

Under a stationarity assumption, we replace B_{t+1} and B_t with B_{MSY} in equation (10) and derive the fishing mortality that maintains B_{MSY}:

$$F_{\mathrm{MSY}} = -\log(1-\phi). \tag{24}$$

Finally, MSY itself is obtained from equation (8), by replacing B_t and F_t with B_{MSY} and F_{MSY}, respectively:

$$\mathrm{MSY} = \frac{\phi}{1-\phi}(1-\phi)^{\frac{1}{\phi}} e^{\rho}. \tag{25}$$

Thus, MSY is a proportion of B_{MSY}, such that the proportionality constant depends only on elasticity:

$$\text{MSY} = \frac{\phi}{1-\phi} B_{\text{MSY}}. \tag{26}$$

Detailed derivation of the above equations is provided in Appendix C.

It is worth noting that the equations for B_{MSY} in the Schaefer and Fox models only depend on carrying capacity (K). For the Pella-Tomlinson and the new model, B_{MSY} also depends on the elasticity parameter ϕ, and thus allows asymmetric responses to depletion (Appendix A.3). This information is critical for management to consider when deciding which model to employ and how much fishing mortality should occur.

2.4 Model fitting and comparison

In order to compare the performance of the novel surplus model against the standard Pella-Tomlinson, Schaefer and Fox approaches, we fit the four models to the Namibian hake data set.

Following the general factorisation of Bayesian hierarchical models, the joint distribution of all state variables and parameters under the three standard models can be found in Parent and Rivot (2012), while for the alternative model it is written as

$$\begin{aligned}[\beta_{1:n}, \phi, \rho, \chi, \sigma | Y_{1:n} = y_{1:n}] \; \propto [\phi] \times [\rho] \times [\chi] \times [\sigma] \times [\beta_1] \times \prod_{t=1}^{n-1} [\beta_{t+1} | \beta_t, \phi, \chi, \sigma] \\ \times \prod_{t=1}^{n} [Y_t = y_t | \beta_t, \rho, \chi, \sigma],\end{aligned} \tag{27}$$

with square brackets denoting densities and n referring to the number of instances. Further

information on this factorisation is available in Wikle et al. (1998) and Clark and Gelfand (2006).

To explore joint posterior distributions of hyperparameters and states, we use Markov chain Monte Carlo methods (MCMC; Gamerman and Lopes, 2006). We employ the software OpenBugs (Thomas et al., 2006) and BRugs (Thomas et al., 2006), the latter being an interface to OpenBugs for `R` (R Core Team, 2014). We deploy three chains, each with a burn-in stage of 10,000 iterations, followed by 1,000,000 iterations thinned at a ratio 1:100. This results in a sample of 10,000 iterations for each chain. Random initial values are generated for all models.

We compare the four models using five types of information: 1) plots of fitted versus observed CPUE indices; 2) plots of biomass estimates; 3) tables with posterior means, variances and cross-correlations of model parameters and reference points; 4) overall goodness-of-fit statistics (Deviance Information Criterion; Spiegelhalter et al., 2002; van der Linde, 2005); 5) MCMC diagnostics (Geweke, 1992; Raftery and Lewis, 1992), available in the `R` package CODA (Plummer et al., 2006); 6) run times of models and sensitivity to initial values. We report results of each model's fastest run time.

To facilitate data exploration, model specification and output analyses, via a graphical user interface, we also developed a package for the software `R`, named `rcsurplus` and located at `www.rcsuite.weebly.com`. Screenshots of the `Shiny` application, included in this package, are provided in Appendix E.

We also compare the four models on two sets of simulated data. The first data set is

simulated using the Schaefer production function, and the second using the new production function. As the results are similar to those found for the Namibian hake data, we only report posterior means and variances of parameter estimates and run times in Appendix F.

3 Results

Nearly all observed CPUE indices fall within the 25th and 75th percentiles of the predictions provided by the four models (Figure 1). Due to slight underestimation of CPUE in 1965 and overestimation in 1967, all models attenuate the fall of CPUE in the first three years of data. Henceforth, posterior medians track changes in CPUE closely.

Biomass estimates are most similar between the new model and the Fox model (Figure 2). However, the new model has more precise estimates, hence smaller confidence intervals. Biomass estimates from Pella-Tomlinson and Schaefer models display more uncertainty than the new and Fox model. Additionally, compared to the Fox and new model, the Schaefer model appears to slightly overestimate biomass, whilst the Pella-Tomlinson model seems to substantially underestimate biomass.

Strong posterior correlations between parameters emerge in all models (Figure 3, D.1, D.2, D.3, D.4). Signs, amplitudes and shapes of correlations are similar between models except the Pella-Tomlinson model. Posterior densities of r, K and q from the Schaefer and Fox models have heavier tails and present greater asymmetry than ϕ, ρ and χ from the new model (Appendix D.1). Also, LOWESS curves fitted to bivariate scatterplots of Schaefer and Fox parameters highlight stronger nonlinearity than the new model as displayed in Figure

3. The posterior distribution of MSY is weakly correlated with K and q in the Schaefer and Fox models, and ρ and χ in the new model. The Pella-Tomlinson model shows strong non-linear relationships between K and q and K and ϕ. However, other relationships do not emerge and considerable noise is present in estimates. This is especially noticeable for the parameter r. MSY is strongly correlated with K, q and ϕ in the Pella-Tomlinson model. Tails also present considerably more breadth in the Pella-Tomlinson model.

Percentiles and moments of posterior distributions are summarized in Table 2. In general, all models provided similar estimates but the new model has less posterior uncertainty for all parameters. Exceptions include large variation in r between the Fox, Schaefer and Pella-Tomlinson models. Also, the Fox model has slightly less uncertainty in reference point estimates than the new model. Additionally, the Pella-Tomlinson model contains more posterior uncertainty in most parameters compared to the other models, along with a substantially higher estimate of ϕ than the new model. Further, the Pella-Tomlinson model estimate of K is substantially lower and more variable than the other models. The new model's increased precision is discernible by comparing standard deviations, percentile ranges and, especially, coefficients of variation. Nevertheless, credibility intervals for equivalent parameters present considerable overlap.

Mean deviance ($\bar{D}_\Theta$) favors the Pella-Tomlinson model: $\bar{D}_\Theta$(Pella-Tomlinson) $= -73.02$, $\bar{D}_\Theta$(new model) $= -46.77$, $\bar{D}_\Theta$(Schaefer) $= -67.69$, $\bar{D}_\Theta$(Fox) $= -68.96$. On the other hand, the effective number of parameters (pD), which should be a positive quantity, cannot be estimated reliably in OpenBUGS, for any model. The alternative estimator of model complexity

(Gelman et al., 2013), $pV = \frac{1}{2}Var(D_\Theta)$, is equally supportive of the new and Fox models: pV(Fox) = 27.05, pV(new model) = 27.05, pV(Schaefer) = 27.28, pV(Pella-Tomlinson) = 27.44. Therefore, based on the Deviance Information Criterion $DIC = \bar{D}_\Theta + pV$, the Pella-Tomlinson model provides a better fit to the data (DIC(Pella-Tomlinson) = -46) than the other models (DIC(new model) = -20, DIC(Schaefer) = -42, DIC(Fox) = -42).

Based on the Geweke test, the new, Schaefer and Fox models converge adequately (Appendix D.1). Specifically, every parameter for each chain passes the Geweke test (i.e., $p > 0.05$). The Pella-Tomlinson model also appears to have adequately converged, except for ϕ, r and q in chain 3, which have absolute Geweke Z-scores over 2 (i.e., $p < 0.05$).

The Raftery and Lewis (1992) statistics also present favorable results for the models (Appendix D.2). The number of iterations required for reliable percentile estimation (N) does not exceed 30,000 for all parameters, except ϕ in chain 1 for the Pella-Tomlinson model (33,105). Additionally, the I statistic (dependence factor) is below 5 for nearly all parameters in all models.

The new model has faster sampling (slowest run took 28 minutes to generate 1,000,000 MCMC iterations), as the other models were between 1.6 to 2.2 times slower, taking an extra 19 to 34 minutes per 1,000,000 iterations (Appendix D.3). These run times reflect the simpler equations employed in the new model, where the posterior distribution of many parameters can be explored via Gibbs sampling instead of Metropolis-Hastings. Moreover, the new model seems to have better mixing and reduced sensitivity to initial values. Samples were performed on a standard laptop (2.53 GHz dual-core processor, 4 GB RAM) running

Windows 7 OS.

4 Discussion and concluding remarks

In this work we compare four hierarchical surplus production models that employ different production functions. The observation equation and the error structure is the same for all models, and so is the data set. Prior distributions are similar (Table 1).

Visual inspection of fits indicates the four models are equally competent at explaining the temporal variability in Namibian hake CPUE (Figure 1). Some lack of fit occurs in the beginning of the time series, a feature that is shared with comparable approaches (Hilborn and Mangel, 1997). Residual uncertainty (σ) is almost identical for the four models (Table 2).

From an implementation standpoint, the new model outperforms existing models. The existing models require a hidden device, which is to truncate estimated biomasses at zero. This procedure is common in fisheries models (Hilborn and Mangel, 1997, pg. 249) but is unfortunate, since it makes results deviate from the error structure assumed in the conceptual model. Such device is not required in the new model, because the model is entirely multiplicative, including the log-normally distributed observation and process errors.

Once logarithms are taken on both sides of the process and observation equations of the new model, two simple expressions result (equations (11) and (13), respectively). This allows the MCMC algorithm to run fast and stable. The joint posterior density of the hyperparameters (ϕ, ρ and χ) is sufficiently close to a multivariate Normal (Figure 3) for

us to postulate that a block Normal proposal density could accelerate model fitting further. Moreover, owing to the linear structure in the new model, efficient exploration of the state $(\beta_t, t = 1, \ldots, n)$ could be performed with the forward filtering, backward sampling algorithm (Frühwirth-Schnatter, 1994), instead of the Gibbs sampler. In the interest of comparing the existing and new model(s) on equal grounds, such attempts are not made here.

Given the uncertainty, the Schaefer, Fox and new model yield similar estimates for reference points relevant to fisheries management: MSY, B_{MSY} and F_{MSY}. The posterior means for MSY fall close to those provided by comparable models in the literature (Hilborn and Mangel, 1997), which include process or observation error, but not both. It is noteworthy that the most complex model fitted by Hilborn and Mangel (1997), which considers lagged recruitment, survival and growth, as well as tight Bayesian prior distributions based on biological information, generates maximum a posteriori estimates of MSY $\approx$ 300 thousand tons). Here we almost replicate those results with the new model, without extra parameters or narrow priors. The Pella-Tomlinson model, on the other hand, provides estimates that differ substantially from other models. The posterior distribution of the additional parameter ϕ appears to be more strongly influenced by the prior than by the likelihood (See Figure D.3 in the Appendix). Hence, we interpret the results from this model with caution.

Strong posterior correlations between hyperparameters emerge in all models. This should not be regarded as a weakness in the models. Rather, it is a consequence of trying to extract diverse information from a single data set, which cannot be controlled through scientific experimentation and contains an untested assumption: that CPUE is proportional to abun-

dance (Hilborn and Mangel, 1997). Our advice, therefore, is that those correlations are taken into account in management strategy evaluation and decision making. Reducing joint posterior densities to products of marginals is, in this case, quite dangerous.

Overall goodness-of-fit statistics (DIC) suggest the Schaefer, Fox, and Pella-Tomlinson models all outperform the new model. However, all models yield negative pD, a symptom of poor model fit (Spiegelhalter et al., 2002). We have explored the impacts of modifying the transformations and bounds for prior densities listed in Table 1, and found that prior information has substantial impact on the DIC. This should not come as a surprise, since only 24 observations are available in the Namibian hake data set. Thus, model comparison might benefit from informative priors that reflect species biology and an understanding of the fishery (Mangel et al., 2013). Our conclusion, which weights this information, the similarity of fitted CPUE indices, residual uncertainty, and the estimates of model complexity proposed by Gelman et al. (2013), is that neither the Schaefer, Fox, or the new model should be discarded as a means to explore Namibian hake population dynamics and fisheries. The Pella-Tomlinson model, on the other hand, appears over-parameterized for this application.

The Schaefer, Fox and Pella-Tomlinson models employ observed catches directly in the original process layer. This excludes fishing effort from entering the model explicitly. We find this feature undesirable, since effort is the input most easily controlled by management. What is more, state-space models typically do not allow observations to enter the process layer directly. Hence, in the new surplus production model, we allow both catchability and effort to enter the process equation, as a surrogate of fishing mortality, and we do not consider

reported catches there.

The faster and more accurate sampling provided by the new model is valuable for fisheries research. Although computations are fast (in the order of minutes) in standard surplus production models, time quickly adds up when moving to more complex models with multiple stocks, additional parameters, and spatial indexation. As an example, the authors have worked with the saucer scallop (*Amusium balloti*) fishery in SE Queensland, Australia, which is typically subdivided into 19 half minute grid cells with specific fishing effort and management. Exploring different parameters for these 19 cells with previous models could take up 20 hours per model run, compared to only 9 hours with the new model. Together with this more economical run time, the new model also offers better accuracy that reduces uncertainty of model output. Overall, this makes the new model a substantial practical improvement.

In summary, the hierarchical state-space model presented in this work constitutes a viable alternative to standard biomass production models. Under a Bayesian setting, we use MCMC methods to fit the model and infer posterior parameter densities. Even with a limited time series of just 24 observations, we avoid setting parameters to constants or introducing narrow priors. The surplus production function stays within the original concept of Pella and Tomlinson (1969), whilst allowing for an asymmetric relationship between biomass and production. Through reparameterisation, we accomplish better MCMC mixing, stability and speed. This work forms the basis for future research, such as age and spatially structured models, where improved parameter estimation and mixing will be valuable.

5 Acknowledgements

Ricardo Lemos received funding for this work from the Australian Fisheries Research and Development Corporation, grant 2013/020. The authors thank Hugh Possingham and Bruno Sansó for useful reviews of preliminary versions of the manuscript. Code sourced from Parent and Rivot (2012) proved invaluable.

References

Andrew, P. A. (1986). Dynamic catch-effort models for the southern african hake populations. Technical Report 10, Benguela Ecology Programme, (CSIR, South Africa).

Berliner, L. M. (1996). *Hierarchical Bayesian time series models*, volume 79 of *Maximum Entropy and Bayesian Methods*. 15th International Workshop on Maximum Entropy and Bayesian Methods, 1995.

Beverton, R. J. H. and Holt, S. J. (1957). On the dynamics of exploited fish populations. *Fishery Investment Series II*, 19:1–533.

Brodziak, J. and Ishimura, G. (2011). Development of Bayesian production models for assessing the north Pacific swordfish population. *Fish. Sci.*, 77(1):22–33.

Brooks, E. N., Powers, J. E., and Cortes, E. (2010). Analytical reference points for age-structured models: application to data-poor fisheries. *ICES J. Mar. Sci.*, 67(1):165–175.

373 Chen, Y. (2003). Quality of fisheries data and uncertainty in stock assessment. *Sci. Mar.*,
374 67:75–87.

375 Clark, J. S. and Gelfand, A. E., editors (2006). *Hierarchical modelling for the environmental*
376 *sciences : statistical methods and applications*. Oxford University Press, Oxford, New
377 York.

378 Conn, P. B., Williams, E. H., and Shertzer, K. W. (2010). When can we reliably estimate
379 the productivity of fish stocks? *Can. J. Fish. Aquat. Sci.*, 67(3):511–523.

380 Cook, R. M. (2013). A fish stock assessment model using survey data when estimates of
381 catch are unreliable. *Fish. Res.*, 143:1–11.

382 Fletcher, R. I. (1978). On restructuring of Pella-Tomlinson system. *Fish. Bull.*, 76(3):515–
383 521.

384 Fox, W. W. (1970). An exponential surplus-yield model for optimizing exploited fish popu-
385 lations. *Trans. Am. Fish. Soc.*, 99(1):80–88.

386 Frühwirth-Schnatter, S. (1994). Data augmentation and dynamic linear models. *J. Time*
387 *Ser. Anal.*, 15(2):183–202.

388 Gamerman, D. and Lopes, H. (2006). *Markov Chain Monte Carlo: Stochastic Simulation for*
389 *Bayesian Inference, Second Edition*. Chapman & Hall/CRC Texts in Statistical Science.
390 Taylor & Francis.

391 Gelman, A., Carlin, J., Stern, H., Dunson, D., Vehtari, A., and Rubin, D. (2013). *Bayesian*

Data Analysis, Third Edition. Chapman & Hall/CRC Texts in Statistical Science. Taylor & Francis.

Geweke, J. (1992). Evaluating the accuracy of sampling-based approaches to the calculation of posterior moments. In J. M. Bernardo, J. 0. Berger, A. P. D. and Smith, A. F. M., editors, *Bayesian Statistics 4*, pages 169–193. Oxford University Press, Oxford.

Glaser, S. M., Ye, H., Maunder, M., MacCall, A., Fogarty, M., and Sugihara, G. (2011). Detecting and forecasting complex nonlinear dynamics in spatially structured catch-per-unit-effort time series for north pacific albacore (*Thunnus alalunga*). *Can. J. Fish. Aquat. Sci.*, 68(3):400–412.

Gould, W. R. and Pollock, K. H. (1997). Catch-effort maximum likelihood estimation of important population parameters. *Can. J. Fish. Aquat. Sci.*, 54(4):890–897.

Gould, W. R., Stefanski, L. A., and Pollock, K. H. (1997). Effects of measurement error on catch-effort estimation. *Can. J. Fish. Aquat. Sci.*, 54(4):898–906.

Graham, M. (1935). Modern theory of exploiting a fishery, and application to north sea trawling. *J. Conseil*, 10(3):264–274.

He, X., Ralston, S., and MacCall, A. D. (2011). Interactions of age-dependent mortality and selectivity functions in age-based stock assessment models. *Fish. Bull.*, 109(2):198–216.

Hilborn, R. (2001). Calculation of biomass trend, exploitation rate, and surplus production from survey and catch data. *Can. J. Fish. Aquat. Sci.*, 58(3):579–584.

411 Hilborn, R. and Mangel, M. (1997). The ecological detective. confronting models with data.
412 *Monographs in Population Biology*, 28:i–xvii, 1–315.

413 Hilborn, R. and Walters, C. J. (1992). *Quantitative Fisheries Stock Assessment: Choice,*
414 *Dynamics and Uncertainty*. Routledge, Chapman and Hall, New York, USA.

415 ICSEAF (1986). Historical series data selected for cape hake assessment. Technical Report
416 89(3), International Commission for the South-East Atlantic Fisheries.

417 Kuparinen, A., Mantyniemi, S., Hutchings, J. A., and Kuikka, S. (2012). Increasing biological
418 realism of fisheries stock assessment: towards hierarchical Bayesian methods. *Environ.*
419 *Rev.*, 20(2):135–151.

420 Lee, H.-H., Maunder, M. N., Piner, K. R., and Methot, R. D. (2012). Can steepness of the
421 stock-recruitment relationship be estimated in fishery stock assessment models? *Fish.*
422 *Res.*, 125:254–261.

423 Ludwig, D. and Walters, C. J. (1981). Measurement errors and uncertainty in parameter
424 estimates for stock and recruitment. *Can. J. Fish. Aquat. Sci.*, 38(6):711–720.

425 Magnusson, A. and Hilborn, R. (2007). What makes fisheries data informative? *Fish Fish.*,
426 8(4):337–358.

427 Mangel, M., MacCall, A. D., Brodziak, J., Dick, E. J., Forrest, R. E., Pourzand, R., and
428 Ralston, S. (2013). A perspective on steepness, reference points, and stock assessment.
429 *Can. J. Fish. Aquat. Sci.*, 70(6):930–940.

McAllister, M. K. and Kirkwood, G. P. (1998). Bayesian stock assessment: a review and example application using the logistic model. *ICES J. Mar. Sci.*, 55(6):1031–1060.

Megrey, B. A. and Wespestad, V. G. (2013). *A review of Biological Assumptions Underlying Fishery Assessment Models*, pages 31–69. Springer-Verlag.

Needle, C. L. (2002). Recruitment models: diagnosis and prognosis. *Rev. Fish Biol. Fish.*, 11(2):95–111.

Parent, E. and Rivot, E. (2012). *Introduction to Hierarchical Bayesian Modeling for Ecological Data*. Chapman and Hall/CRC, USA.

Pella, J. J. and Tomlinson, P. K. (1969). A generalised stock production model. *Bull. - Inter-Am. Trop. Tuna Comm.*, 13:421–458.

Plummer, M., Best, N., Cowles, K., and Vines, K. (2006). CODA: Convergence diagnosis and output analysis for MCMC. *R News*, 6(1):7–11.

Polacheck, T., Hilborn, R., and Punt, A. E. (1993). Fitting surplus production models - comparing methods and measuring uncertainty. *Can. J. Fish. Aquat. Sci.*, 50(12):2597–2607.

Punt, A. E. and Szuwalski, C. (2012). How well can F_{MSY} and B_{MSY} be estimated using empirical measures of surplus production? *Fish. Res.*, 134:113–124.

Quinn, II, T. J. and Deriso, R. B. (1999). *Quantitative fish dynamics*. Oxford University Press, New York, USA.

R Core Team (2014). *R: A Language and Environment for Statistical Computing*. R Foundation for Statistical Computing, Vienna, Austria.

Raftery, A. E. and Lewis, S. M. (1992). One long run with diagnostics: Implementation strategies for Markov Chain Monte Carlo. *Stat. Sci.*, 7(4):493–497.

Rivard, D. and Bledsoe, L. J. (1978). Parameter-estimation for Pella-Tomlinson stock production-model under non-equilibrium conditions. *Fish. Bull.*, 76(3):523–534.

Rose, K. A. and Cowan, J. H. (2003). Data, models, and decisions in US marine fisheries management: Lessons for ecologists. *Annu. Rev. Ecol. Evol. Syst.*, 34:127–151.

Schaefer, M. B. (1954). Some aspects of the dynamics of populations important to the management of the commercial marine fisheries. *Bull. - Inter-Am. Trop. Tuna Comm.*, 1(1-2):27–56.

Schnute, J. T. and Richards, L. J. (2001). Use and abuse of fishery models. *Can. J. Fish. Aquat. Sci.*, 58(1):10–17.

Spiegelhalter, D. J., Best, N. G., Carlin, B. R., and van der Linde, A. (2002). Bayesian measures of model complexity and fit. *J. R. Stat. Soc. Ser. B-Stat. Methodol.*, 64:583–616.

Thomas, A., O'Hara, B., Ligges, U., and Sturtz, S. (2006). Making bugs open. *R News*, 6(1):12–17.

Uhler, R. S. (1980). Least-squares regression estimates of the Schaefer production-model - some Monte-Carlo simulation results. *Can. J. Fish. Aquat. Sci.*, 37(8):1284–1294.

van der Linde, A. (2005). DIC in variable selection. *Stat. Neerl.*, 59(1):45–56.

Verhulst, P. F. (1838). Notice sur la loi que la population suit dans son accroissement. *Corresp. Math. Phys.*, 10:113–121.

Walters, C. and Ludwig, D. (1994). Calculation of Bayes posterior probability-distributions for key population parameters. *Can. J. Fish. Aquat. Sci.*, 51(3):713–722.

Wang, S.-P., Maunder, M. N., and Aires-da Silva, A. (2009). Implications of model and data assumptions: An illustration including data for the Taiwanese longline fishery into the eastern Pacific ocean bigeye tuna (*Thunnus oblesus*) stock assessment. *Fish. Res.*, 97(1-2):118–126.

Wang, S.-P., Maunder, M. N., and da Silva, A. A. (2014). Selectivity's distortion of the production function and its influence on management advice from surplus production models. *Fish. Res.*, 158:181 – 193.

Wikle, C. K., Berliner, L. M., and Cressie, N. (1998). Hierarchical Bayesian space-time models. *Environ. Ecol. Stat.*, 5(2):117–154.

Xiao, Y. S. (1998). Two simple approaches to use of production models in fish stock assessment. *Fish. Res.*, 34(1):77–86.

Zhang, Z. (2013). Evaluation of logistic surplus production model through simulations. *Fish. Res.*, 140:36–45.

6 Tables

Table 1: Priors for hyperparameters in the Schaefer and Fox models (left column), the Pella-Tomlinson model (center column) and the new model (right column).

Schaefer and Fox	Pella-Tomlinson	New model
$K \sim \text{Uniform}[100, 15000]$	$K \sim \text{Uniform}[100, 15000]$	$e^{\rho} \sim \text{Uniform}[100, 15000]$
$\log(q) \sim \text{Uniform}[-20, -3]$	$\log(q) \sim \text{Uniform}[-20, -3]$	$\chi \sim \text{Uniform}[-20, -3]$
$r \sim \text{Uniform}[0.01, 3]$	$r \sim \text{Uniform}[0.01, 3]$	
	$\phi \sim \text{Uniform}[0, 1]$	$\phi \sim \text{Uniform}[0, 1]$
$\log(\sigma) \sim \text{Uniform}[-20, -1]$	$\log(\sigma) \sim \text{Uniform}[-20, 1]$	$\log(\sigma) \sim \text{Uniform}[-20, -1]$

Table 2: Posterior means, standard deviations, coefficients of variation and percentiles for model parameters and MSY quantities, under the four models (Schaefer, Fox, Pella-Tomlinson and new).

model	parameter	mean	st. dev.	c.v.	2.5%	median	97.5%
Schaefer	r	0.277	0.123	0.44	0.058	0.276	0.521
	K	4771	2568	0.54	2212	3902	12550
	q	0.00034	0.00012	0.37	0.00012	0.00034	0.00058
	σ	0.0096	0.0034	0.35	0.0051	0.009	0.018
	B_{MSY}	2385	1284	0.54	1106	1951	6274
	F_{MSY}	0.139	0.061	0.44	0.029	0.138	0.261
	MSY	267	55	0.21	142	269	370
Fox	r	1.471	0.532	0.36	0.422	1.481	2.497
	K	4632	2243	0.48	2380	3935	11640
	q	0.00035	0.00011	0.33	0.00013	0.00035	0.00057
	σ	0.0089	0.0031	0.35	0.0047	0.0083	0.0166
	B_{MSY}	1704	825.3	0.48	875.5	1448	4282
	F_{MSY}	0.179	0.071	0.39	0.046	0.179	0.32
	MSY	258	48	0.19	155	260	346
Pella-Tomlinson	r	0.169	0.059	0.35	0.07	0.162	0.304

model	parameter	mean	st. dev.	c.v.	2.5%	median	97.5%
	K	2957	3488	1.18	382.6	1235	12870
	q	0.00152	0.00126	0.83	0.00012	0.00121	0.00422
	ϕ	0.339	0.302	0.89	0.019	0.236	0.956
	σ	0.0074	0.0026	0.35	0.004	0.0069	0.0139
	B_{MSY}	1139	1283	1.13	185.1	504.1	4788
	F_{MSY}	0.127	0.036	0.29	0.058	0.126	0.201
	MSY	149	183	1.23	15	64	678
New	ϕ	0.184	0.07	0.38	0.052	0.182	0.328
	e^{ρ}	4399	2048	0.47	2268	3817	10590
	e^{χ}	0.00037	0.00012	0.32	0.00014	0.00037	0.0006
	σ	0.0094	0.0032	0.34	0.005	0.0088	0.0173
	B_{MSY}	1480	760.1	0.51	680.2	1266	3784
	F_{MSY}	0.207	0.088	0.43	0.054	0.201	0.397
	MSY	283	55	0.2	165	284	387

7 List of figures

Figure 1: Time series of observed CPUE (black dots connected by line), together with posterior medians (horizontal dashes in boxes), first and third quartiles (boxes), and 2.5/97.5 percentiles (whiskers), provided by (from left to right. light grey to dark grey) the new, Schaefer, Fox and Pella-Tomlinson models.

Figure 2: Time series of biomass estimate posterior medians (horizontal dashes in boxes), first and third quartiles (boxes), and 2.5/97.5 percentiles (whiskers), provided by (from left to right; light grey to dark grey) the new, Schaefer, Fox and Pella-Tomlinson models.

Figure 3: Joint posterior distribution of parameters ϕ, ρ and χ, as well as MSY, in the new model. Marginal densities are on the diagonal, Pearson correlation estimates above, and scatter plots of MCMC variates, with locally weighted scatterplot smoothing (LOWESS) curves, below.

8 Figures

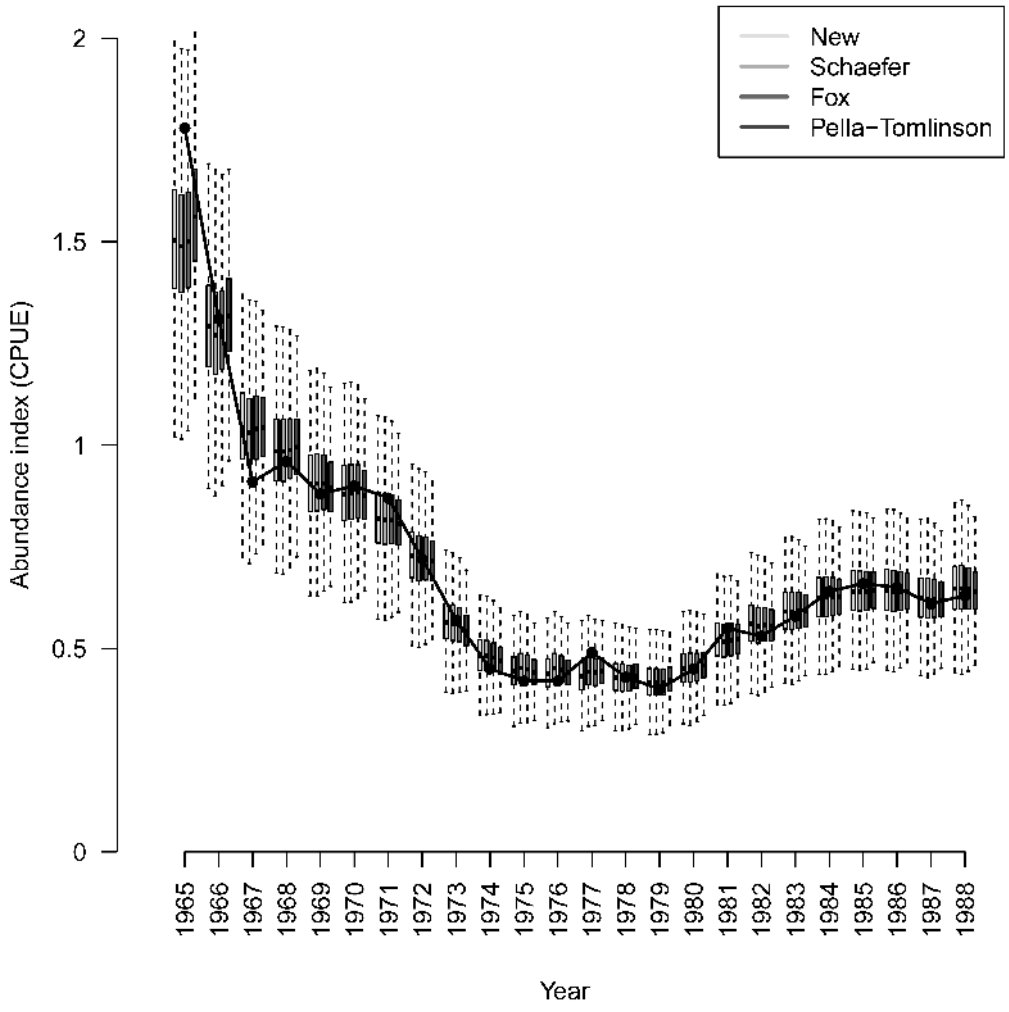

Figure 1: Time series of observed CPUE (black dots connected by line), together with posterior medians (horizontal dashes in boxes), first and third quartiles (boxes), and 2.5/97.5 percentiles (whiskers), provided by (from left to right) the new, Schaefer, Fox and Pella-Tomlinson models.

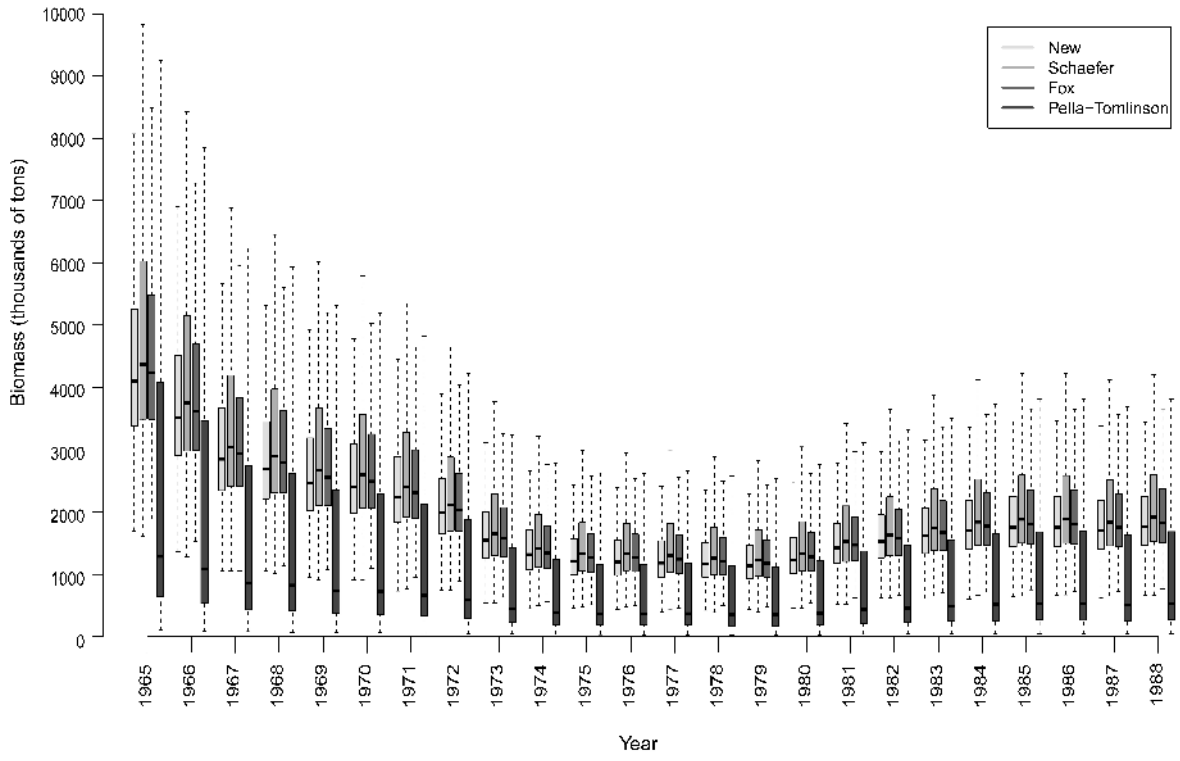

Figure 2: Time series of biomass estimate posterior medians (horizontal dashes in boxes), first and third quartiles (boxes), and 2.5/97.5 percentiles (whiskers), provided by (from left to right; light grey to dark grey) the new, Schaefer, Fox and Pella-Tomlinson models.

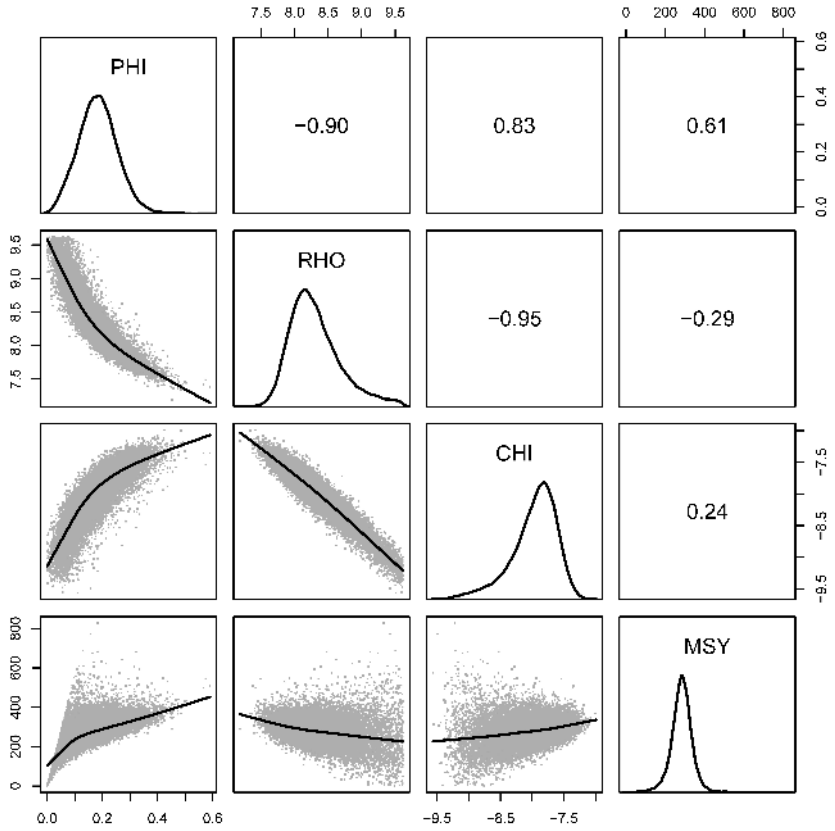

Figure 3: Joint posterior distribution of parameters ϕ, ρ and χ, as well as MSY, in the new model. Marginal densities are on the diagonal, Pearson correlation estimates above, and scatter plots of MCMC variates, with locally weighted scatterplot smoothing (LOWESS) curves, below.

A The alternative process equation

A.1 Derivation

We start from the typical difference equation (Parent and Rivot, 2012) that characterises the evolution of an exploited population, in terms of its biomass (B_t):

$$B_{t+1} = B_t + h(B_t) - C_t. \tag{1}$$

In this equation, the production function $h(B_t)$ provides an estimate of biomass growth given its current level. Total catch, C_t, is assumed to occur after production and be only partly observable, since it includes reported and unreported catches, as well as discards. Hence, a novel and alternative way to write catch is,

$$C_t = \left(1 - e^{-F_t}\right) \times \left(B_t + h(B_t)\right), \tag{2}$$

where F_t designates the fishing mortality rate at time t. By replacing C_t in equation (1) with the right-hand side of equation (2), we obtain

$$B_{t+1} = B_t + h(B_t) - [(1 - e^{-F_t})(B_t + h(B_t))], \tag{3}$$

which can be simplified to

$$\begin{aligned} B_{t+1} &= B_t + h(B_t) - B_t - h(B_t) + \left(B_t + h(B_t)\right) e^{-F_t} \\ &= \left(B_t + h(B_t)\right) e^{-F_t}. \end{aligned} \tag{4}$$

We propose a novel production function $h(B_t)$, defined as

$$h(B_t) = \frac{r_t}{\phi} B_t \left(1 - \left(\frac{B_t}{K}\right)^{\phi}\right), \tag{5}$$

where r_t is the intrinsic rate of population growth at time t, K is the carrying capacity of the environment and ϕ is a shape parameter. We let r_t be a function of depletion ratio and shape parameter ϕ:

$$r_t = \phi \left(\frac{B_t}{K}\right)^{-\phi}. \tag{6}$$

With equation (6), equation (5) becomes

$$\begin{aligned} h(B_t) &= \left(\frac{B_t}{K}\right)^{-\phi} B_t \left(1 - \left(\frac{B_t}{K}\right)^{\phi}\right) \\ &= \left(\frac{B_t}{K}\right)^{-\phi} \left(B_t - \frac{B_t^{1+\phi}}{K^{\phi}}\right) \\ &= \frac{B_t^{1-\phi}}{K^{-\phi}} - B_t \\ &= B_t^{1-\phi} K^{\phi} - B_t. \end{aligned} \tag{7}$$

Finally, with the last expression in equation (7), equation (4) simplifies to

$$\begin{aligned} B_{t+1} &= \left(B_t + B_t^{1-\phi} K^{\phi} - B_t\right) e^{-F_t} \\ &= B_t^{1-\phi} K^{\phi} e^{-F_t} \end{aligned} \tag{8}$$

A.2 Log-transformation

Applying the logarithmic function on both sides of equation (8) yields

$$\log(B_{t+1}) = (1-\phi)\log(B_t) + \phi \log(K) - F_t. \tag{9}$$

Define $\rho = \log(K)$ as the log-carrying capacity; write

$$\begin{aligned} \beta_t &= \log\left(\frac{B_t}{K}\right) \\ &= \log(B_t) - \rho \end{aligned}$$

as the scaled and log-transformed biomass. With this new set of variables, equation (9) becomes

$$\beta_{t+1} + \rho = (1 - \phi) \times (\beta_t + \rho) + \phi\rho - F_t$$

$$\Leftrightarrow \qquad \beta_{t+1} = (1 - \phi)\beta_t - F_t. \tag{10}$$

We assume that fishing mortality rate F_t follows a Normal distribution, $F_t \sim N[qE_t, \sigma]$. The mean comprises a product of catchability (q, unknown) and fishing effort (E_t, known). The variance (σ) is an unknown hyperparameter. With this expression for F_t and $\chi = \log(q)$ as the log-catchability parameter, equation (10) becomes

$$\beta_{t+1} = (1 - \phi)\beta_t - e^{\chi}E_t + \epsilon_t, \tag{11}$$

where $\epsilon_t \sim N[0, \sigma]$.

A.3 Analysis of the production function

Here we compare three production functions ($h(B)$): logistic (Verhulst, 1838; Schaefer, 1954), Gompertz (Fox, 1970) and the new function. In Figure A.1 we explore the shape of the new production function, which assumes that productivity is higher at low to medium population levels. Depending on the value of the elasticity, asymmetry with respect to an imaginary vertical line placed at the 50% depletion ratio can be higher ($\phi \to 1$) or lower ($\phi \to 0$). Hence, low values of ϕ make populations more susceptible to crashes, if a substantial fraction of the original biomass is removed. In contrast, high values for ϕ allow larger amounts of biomass to be removed consistently, because populations can rejuvenate at comparable pace.

The logistic (Figure A.2) function, in contrast, does not possess asymmetry in production rates. Populations are expected to produce their peak amount of productivity at half the carrying capacity (K). The Gompertz (Figure A.3) function allows slightly more asymmetry in production, with the peak below 50% of the carrying capacity, but this is marginal in comparison to the new approach.

A.4 References

Fox, W. W. (1970). An exponential surplus-yield model for optimizing exploited fish populations. *Trans. Am. Fish. Soc.*, 99(1):80–88.

Parent, E. and Rivot, E. (2012). *Introduction to Hierarchical Bayesian Modeling for Ecological Data*. Chapman and Hall/CRC, USA.

Schaefer, M. B. (1954). Some aspects of the dynamics of populations important to the management of the commercial marine fisheries. *Bull. - Inter-Am. Trop. Tuna Comm.*, 1(1-2):27–56.

Verhulst, P. F. (1838). Notice sur la loi que la population suit dans son accroissement. *Corresp. Math. Phys.*, 10:113–121.

B Log-transformation of the observation equation

Suppose a time series of catch per unit effort (i_t, $t = 1, \ldots, n$) is available. In line with standard approaches, we assume this index to be proportional to biomass (B_t), that is, $i_t = qB_t, \forall_{t\in(1,\cdots,n)}$, with q denoting the catchability parameter. Parent and Rivot (2012), among others, build upon this structure by introducing log-normally distributed error (ω_t), to obtain the stochastic observation equation

$$i_t = qB_t e^{\omega_t}. \tag{12}$$

Using the reparameterization employed in the process layer — i.e., $\chi = \log(q)$, $\beta_t = \log(B_t/K)$ and $\rho = \log(K)$, where K represents the carrying capacity —, equation (12) can also be written as

$$\begin{aligned} i_t &= (e^{\chi}) \times (e^{\beta_t+\rho}) \times (e^{\omega_t}) \\ \Leftrightarrow i_t &= e^{\chi+\beta_t+\rho+\omega_t}. \end{aligned}$$

With $Y_t = \log(i_t)$ denoting the observed log-CPUE index, and applying the logarithmic function to both sides of this equation, we obtain

$$Y_t = \chi + \beta_t + \rho + \omega_t. \tag{13}$$

B.1 References

Parent, E. and Rivot, E. (2012). *Introduction to Hierarchical Bayesian Modeling for Ecological Data*. Chapman and Hall/CRC, USA.

C Reference points

Here we derive reference points for fisheries management, under the novel surplus production function (derived in equation (7) of Appendix A.1 and discussed further in Appendix A.3):

$$h(B_t) = B_t^{1-\phi} K^{\phi} - B_t \tag{14}$$

where B_t stands for biomass at time t, K is the carrying capacity (also written as e^{ρ}), and ϕ is a shape parameter, which we dub elasticity. As exemplified in Appendix A.3, the production function admits one maximum, when $\phi \in (0, 1)$. To find it, we derive $h(B_t)$ with respect to biomass and equate the result to zero:

$$\begin{aligned}
&\frac{\partial h(B_t)}{\partial B_t} = 0 \\
\Leftrightarrow\ &(1-\phi) B_t^{-\phi} K^{\phi} - 1 = 0 \\
\Leftrightarrow\ &B_t^{-\phi} = \frac{1}{(1-\phi) K^{\phi}} \\
\Leftrightarrow\ &B_t^{\phi} = (1-\phi) K^{\phi} \\
\Leftrightarrow\ &B_t = (1-\phi)^{\frac{1}{\phi}} K
\end{aligned}$$

Hence, the biomass level that maximizes production is

$$B_{\text{MSY}} = (1-\phi)^{\frac{1}{\phi}} K \tag{15}$$

or, equivalently, $B_{\text{MSY}} = (1-\phi)^{1/\phi} e^{\rho}$. We also point out that, by plugging B_{MSY} into the production function, we obtain

$$\begin{aligned} h(B_{\text{MSY}}) &= B_{\text{MSY}}^{1-\phi} K^{\phi} - B_{\text{MSY}} \\ &= (1-\phi)^{\frac{1-\phi}{\phi}} K - (1-\phi)^{\frac{1}{\phi}} K \\ &= (1-\phi)^{\frac{1-\phi}{\phi}} \left(1 - (1-\phi)\right) K \\ &= \phi (1-\phi)^{\frac{1-\phi}{\phi}} K. \end{aligned}$$

The fishing mortality rate that maintains B_{MSY} is F_{MSY}. We can derive it from the process equation (see Appendix A.1)

$$B_{t+1} = B_t^{1-\phi} K^{\phi} e^{-F_t},$$

by replacing B_{t+1} and B_t with the newly found formula for B_{MSY} (equation (15)):

$$\begin{aligned} & B_{\text{MSY}} = B_{\text{MSY}}^{1-\phi} K^{\phi} e^{-F_t} \\ \Leftrightarrow\ & (1-\phi)^{\frac{1}{\phi}} K = \left((1-\phi)^{\frac{1}{\phi}} K \right)^{1-\phi} K^{\phi} e^{-F_t} \\ \Leftrightarrow\ & (1-\phi)^{\frac{1}{\phi}} K = (1-\phi)^{\frac{1-\phi}{\phi}} K e^{-F_t} \\ \Leftrightarrow\ & (1-\phi)^{\frac{1}{\phi} - \frac{1-\phi}{\phi}} = e^{-F_t} \\ \Leftrightarrow\ & (1-\phi) = e^{-F_t} \\ \Leftrightarrow\ & \log(1-\phi) = -F_t \end{aligned}$$

559 Thus, we reach a simple expression for F_{MSY}:

$$F_{\text{MSY}} = -\log(1-\phi). \tag{16}$$

To get the expression for Maximum Sustainable Yield start from the catch equation (2)

$$C_t = \left(1 - e^{-F_t}\right) \times \left(B_t + h(B_t)\right),$$

where we replace B_t and F_t with B_{MSY} and F_{MSY}, respectively. We obtain

$$\begin{aligned}
C_t &= \left(1 - e^{-F_{\text{MSY}}}\right) \times \left(B_{\text{MSY}} + h(B_{\text{MSY}})\right) \\
&= \left(1 - e^{\log(1-\phi)}\right) \times \left(B_{\text{MSY}} + B_{\text{MSY}}^{1-\phi} K^{\phi} - B_{\text{MSY}}\right) \\
&= \phi B_{\text{MSY}}^{1-\phi} K^{\phi} \\
&= \phi(1-\phi)^{\frac{1}{\phi}-1} K \\
&= \frac{\phi}{1-\phi}(1-\phi)^{\frac{1}{\phi}} K.
\end{aligned}$$

Therefore, MSY is a proportion of B_{MSY}, such that the proportionality constant only depends on elasticity:

$$\text{MSY} = \frac{\phi}{1-\phi} B_{\text{MSY}}. \tag{17}$$

D Model comparison

D.1 Posterior distributions

In this section, we present and compare the posterior densities for the parameters in the Schaefer, Fox, Pella-Tomlinson and new models. Specifically, K and q in figures D.1 D.2 D.3 are analogous to e^{ρ} and e^{χ} in figure D.4. Examining the two figures, it is apparent the models have similar posterior correlations between parameters.

Figure D.5 compares the MSY estimates of the Schaefer, Fox, Pella-Tomlinson and new model. The Schaefer and new model peak to the right of the Pella-Tomlinson and Fox models, thereby becoming closer to estimates produced by Hilborn and Mangel (1997).

D.2 Convergence diagnostics

Here we present convergence diagnostics for the four models, estimated using default options in the CODA package (Plummer et al., 2006). The Geweke (1992) diagnostic consists of a Z-score, obtained from a comparison between the first 10% of a Markov chain and the last 50%. A significant difference ($p < 0.05$) indicates the parameter may not have converged for that chain. From Table D.1 it is apparent all parameters converged in all three chains for the new, Schaefer and Fox models. The Pella-Tomlinson model also appears to have adequately converged, except for ϕ, r and q in chain 3 which have absolute Geweke Z-scores over 2 (i.e., $p < 0.05$). Overall, this indicates the four models can be considered to have reliable results, though there is slight uncertainty with some parameters for the Pella-Tomlinson model.

Raftery and Lewis (1992) statistics (quantile = 2.5%, accuracy ±0.005, probability of attainment = 0.95) are presented in Table D.2. For an indication of good mixing and convergence, according to this diagnostic, the dependence factor (I) should be below 5, and the total number of MCMC iterations required (N) should be less than 30000. From Table D.2 it is apparent nearly all parameters have $I < 5$. Exceptions are χ in the new model, which has an I that marginally ranges above 5 (5.13 to 6.15). Also, r has an I of 5.76 and q 6.53 for chains 1 and 3, respectively, for the Fox model. Whilst for the Pella-Tomlinson model, I for ϕ is 8.84 and 6.11 for chains 1 and 2 respectively, whilst I for q is 6.46 and 6.86 for chains 1 and 3 respectively. The number of iterations required for reliable percentile estimation (N) does not exceed 30,000 for all parameters, except ϕ in chain 1 for the Pella-Tomlinson model (33,105).

Overall, since we are conducting many tests, we expect to reject a few spuriously, and therefore we find no reason to believe that any model failed at large to converge in their respective parameters.

D.3 Model sampling times

From Table D.3 it is apparent the new model has faster sampling (slowest 28 minutes per 1,000,000 iterations), as the other models were between 1.6 to 2.2 times slower, taking an extra 19 to 34 minutes per 1,000,000 iterations (Appendix D.3).

D.4 References

Geweke, J. (1992). Evaluating the accuracy of sampling-based approaches to the calculation of posterior moments. In J. M. Bernardo, J. 0. Berger, A. P. D. and Smith, A. F. M., editors, *Bayesian Statistics 4*, pages 169–193. Oxford University Press, Oxford.

Hilborn, R. and Mangel, M. (1997). The ecological detective. confronting models with data. *Monographs in Population Biology*, 28:i–xvii, 1–315.

Plummer, M., Best, N., Cowles, K., and Vines, K. (2006). CODA: Convergence diagnosis and output analysis for MCMC. *R News*, 6(1):7–11.

Raftery, A. E. and Lewis, S. M. (1992). One long run with diagnostics: Implementation strategies for Markov Chain Monte Carlo. *Stat. Sci.*, 7(4):493–497.

E A package for R

Together with this manuscript, we have developed an `R` package `rcsurplus` to facilitate the comparison of the new surplus production model with the canonical models. The package contains a single function, `rcsurplus_gui()`, which deploys a Shiny application on the user's web browser. In this app, the user can visually inspect the Namibian hake data set (Figure E.1), specify model priors and MCMC parameters (Figure E.2), and analyse convergence diagnostics and model fits (Figure E.3).

F Simulated data analysis

Here we present results for the four models on two sets of simulated data. The first data set is generated using the Schaefer equation (4), and the second using the new production equation (10). The true values for the parameters are presented in Table F.1 and the simulated data in Table F.2. As the results are similar to those found for the Namibian hake data, we only report posterior means and variances of parameter estimates and run times in Tables F.3 and F.4 for Simulation 1, and Tables F.5 and F.6 for Simulation 2.

We fit the four models (Schaefer, Fox, Pella-Tomlinson and new model) as we did for the hake data: i) for each model, we implement three runs of three randomly initiated chains; ii) each chain has a burn in of 10,000 iterations, followed by 1,000,000 iterations; iii) we keep every hundredth iteration for a total sample size of 30,000 iterations per run; iv) we report parameter estimates in Tables F.3 and F.5), for the fastest run times indicated by bold text in Tables F.4 and F.6.

We examine how well the models predict Simulation 1 data by comparing posterior mean estimates (Table F.3) to true parameter values (Table F.1). The Schaefer and new model come close to predicting the true parameter values, whilst the Fox and Pella-Tomlinson do not perform nearly as well. Posterior means of the Schaefer model underestimate r by 19%, q by 7% and overestimate K by 8% and σ by 14%. The new model's posterior means underestimate e^{χ} by 9% and overestimate e^{ρ} by 9% and σ by 39%. Posterior means for the Fox model overestimate r by 103%, K by 19% and σ by 22%, whilst underestimating q by 16%. The Pella-Tomlinson model overestimates K by 213%, q by 124%, σ by 323% and

underestimates r by 91%.

Overall, the Schaefer and new model show good accuracy; all parameters are in the 2.5% and 97.5% percentile range. The Fox and Pella-Tominlon models have noticeable errors in parameter estimates. The Fox model is unable to place any parameters except σ between the 2.5% and 97.5% percentile ranges. The Pella-Tomlinson model only places K between the 2.5% and 97.5% percentile ranges but with variation ranging from 89 to 1253% of the true value.

Coefficients of variation are similar for the Schaefer, Fox and new model, and are much smaller in comparison to those of the Pella-Tomlinson model. For example, the Pella-Tomlinson model has 12 and 15 times the coefficient of variation for K (e^{ρ}) and q (e^{χ}), respectively, than the other models.

Examining run times, the new model easily outperforms the other models (Table F.4). The new model is able to complete sampling in 31 minutes. This is twice to 2.6 times as quick as the other models' fastest run time. The other models performed consistently, with the Schaefer model being the next fastest at 64 minutes, Fox at 74 minutes and Pella-Tomlinson at 82 minutes.

These results are relatively simple to interpret. First, we expect the Schaefer model to have better performance, as it was used to simulate the data. Biomass dynamics follow the Schaefer model's process equation and thus estimated parameters should be close to true values. Second, the new model performs well because it has sufficient flexibility in the production function to approximate the Schaefer production function. It also has a linear

structure which improves the sampling speed. Third, the Fox production function has a shape different to the Schaefer model, and so it would not be expected to accurately predict parameter values for a population that follows the Schaefer production function. Finally, the more complex Pella-Tomlinson model could not approximate a shape similar to the Schaefer production function, probably because it is overparameterized relative to the data provided.

We now examine how well the models predict the data generated according to Simulation 2, by comparing parameter mean estimates (Table F.5) to true parameter values (Table F.1). The Fox and new model come close to predicting the true parameter values, whilst the Schaefer and Pella-Tomlinson do not perform nearly as well. The new model overestimates ϕ by 21% and underestimates e^{χ} by 12%, e^{ρ} by 31% and σ by 3%. The Fox model underestimates K by 17% and q by 26%, whilst underestimating q by 26% and σ by 28%. The Pella-Tomlinson model overestimates K by 145%, q by 59%, σ by 42% and underestimate ϕ by 21%. The Schaefer model overestimates σ by 8392%, K by 166% and q by 820%.

Overall, the Fox and new model show good accuracy; the true value of all parameters except K (e^{ρ}), and q for the Fox model, are in the 2.5% and 97.5% percentile range. The Schaefer and Pella-Tominlon models capture the true value of all parameters between the 2.5% and 97.5% percentile ranges, but have noticeable difficulties in assessing uncertainty. For example, in The Schaefer model, the 95% credibility interval for K ranges from 29% to 1091% of the true value; for the Pella-Tomlinson model, the range is from 88% to 1170%.

Coefficients of variation are similar for the Fox and new model, and are much smaller in comparison to those of the Pella-Tomlinson and Schaefer model. For example, the Schaefer

and Pella-Tomlinson model have 14 and 16 times the coefficient of variation for K (e^{ρ}) than the other models.

Examining run times, the new model easily outperforms the other models (Table F.6). The new model is able to complete the sampling in 33 minutes. This is 1.8 to 2.5 times as quick as the other models' fastest run time. The other models performed consistently, with the Schaefer model being the next fastest at 59 minutes, Fox at 76 minutes and Pella-Tomlinson at 84 minutes.

These results are also relatively straightforward to interpret. First, we expect the new model to have better performance, since its production function was used to simulate the data. The biomass dynamics follow the model's process equation and thus estimated parameters should fall close to true values. The new model also has a linear structure, which improves sampling speed. Second, we expect the Fox model to estimate parameters correctly, given that the Fox production function has a shape similar to the new production function, when $\phi = 0.3$. Third, we anticipate the opposite behavior in the Schaefer model, since the shape of its production function differs from that used in simulating the data. Finally, as before, the more complex Pella-Tomlinson model cannot estimate parameters reliably, as it is likely the data set has insufficient information, namely to separate ϕ from r.

In summary, the simulations confirm and strengthen the results of the Namibian hake data analysis. The new model samples faster and has similar accuracy to the best existing surplus production model for the data at hand. Moreover, it seems more flexible than the other models, including the overparameterized Pella-Tomlinson, to adjust to different "true"

surplus production functions. Thus, the new model may be applicable to a broader range of data sets than the other three models.

G Appendix tables

Table D.1: Geweke convergence diagnostics, Z score and associated p-value in parenthesis (significant values are bold), for the three chains of r, K, q, σ (Schaefer and Fox), ϕ, r, K, q, σ (Pella-Tomlinson) and ϕ, e^{ρ}, χ, σ (new model).

Model	Parameter	Chain 1	Chain 2	Chain 3
Schaefer	r	-0.008 (0.994)	0.013 (0.99)	1.306 (0.192)
	K	0.071 (0.943)	-0.227 (0.82)	-1.143 (0.253)
	$\log(q)$	0.169 (0.866)	0.043 (0.966)	1.337 (0.181)
	$\log(\sigma)$	-0.794 (0.427)	0.436 (0.663)	-0.838 (0.402)
Fox	r	-1.81 (0.07)	-1.019 (0.308)	0.512 (0.609)
	K	1.33 (0.184)	0.836 (0.403)	-0.441 (0.659)
	$\log(q)$	-1.592 (0.111)	-1.054 (0.292)	0.33 (0.741)
	$\log(\sigma)$	1.17 (0.242)	-0.089 (0.93)	-0.213 (0.831)
Pella-Tomlinson	ϕ	0.683 (0.495)	-0.261 (0.794)	-2.197 (**0.028**)
	r	0.567 (0.571)	0.163 (0.871)	-2.316 (**0.021**)
	K	-0.322 (0.747)	0.204 (0.838)	1.227 (0.22)
	$\log(q)$	0.76 (0.447)	-0.278 (0.781)	-1.999 (0.046)
	$\log(\sigma)$	-1.937 (0.053)	-0.647 (0.518)	0.101 (0.92)
New model	ϕ	-1.368 (0.171)	-0.695 (0.487)	-1.508 (0.132)
	e^{ρ}	0.995 (0.32)	0.799 (0.424)	1.801 (0.072)
	χ	-1.125 (0.261)	-0.945 (0.345)	-1.804 (0.071)
	$\log(\sigma)$	0.164 (0.87)	1.437 (0.151)	1.796 (0.072)

Table D.2: Raftery and Lewis (1992) convergence diagnostics for three chains with parameters r, K, q, σ (Schaefer and Fox), ϕ, r, K, q, σ (Pella-Tomlinson) and ϕ, e^{ρ}, χ, σ (new model). Nmin refers to minimum sample size based on zero autocorrelation.

Model	Chain	Parameter	Burn in (M)	Total (N)	Nmin	Dependence factor (I)
Schaefer	Chain 1	r	12	14916	3746	3.98
		K	6	9166	3746	2.45
		$\log(q)$	12	16164	3746	4.32
		$\log(\sigma)$	2	3834	3746	1.02
	Chain 2	r	8	10050	3746	2.68
		K	4	4996	3746	1.33
		$\log(q)$	12	15312	3746	4.09
		$\log(\sigma)$	2	3802	3746	1.01
	Chain 3	r	12	10563	3746	2.82
		K	6	8412	3746	2.25
		$\log(q)$	12	12663	3746	3.38
		$\log(\sigma)$	2	3771	3746	1.01
Fox	Chain 1	r	12	21568	3746	5.76
		K	4	4913	3746	1.31

Model	Chain	Parameter	Burn in (M)	Total (N)	Nmin	Dependence factor (I)
		$\log(q)$	12	16692	3746	4.46
		$\log(\sigma)$	2	3771	3746	1.01
	Chain 2	r	12	15603	3746	4.17
		K	3	4520	3746	1.21
		$\log(q)$	12	13960	3746	3.73
		$\log(\sigma)$	2	3561	3746	0.95
	Chain 3	r	8	11528	3746	3.08
		K	4	4752	3746	1.27
		$\log(q)$	24	24480	3746	6.53
		$\log(\sigma)$	2	3650	3746	0.97
Pella-Tomlinson	Chain 1	ϕ	25	33105	3746	8.84
		r	3	4028	3746	1.08
		K	10	12726	3746	3.4
		$\log(q)$	20	24190	3746	6.46
		$\log(\sigma)$	2	3680	3746	0.98
	Chain 2	ϕ	16	22884	3746	6.11
		r	2	3710	3746	0.99
		K	8	10170	3746	2.71
		$\log(q)$	12	17440	3746	4.66
		$\log(\sigma)$	2	3741	3746	1

Model	Chain	Parameter	Burn in (M)	Total (N)	Nmin	Dependence factor (I)
	Chain 3	ϕ	9	12510	3746	3.34
		r	4	6762	3746	1.81
		K	10	12304	3746	3.28
		$\log(q)$	20	21955	3746	5.86
		$\log(\sigma)$	2	3741	3746	1
New model	Chain 1	ϕ	15	13734	3746	4.37
		e^{ρ}	4	5187	3746	1.38
		χ	21	23043	3746	6.15
		$\log(\sigma)$	2	3650	3746	0.97
	Chain 2	ϕ	10	11112	3746	2.97
		e^{ρ}	4	4832	3746	1.29
		χ	15	20043	3746	5.35
		$\log(\sigma)$	2	3771	3746	1.01
	Chain 3	ϕ	10	11070	3746	2.96
		e^{ρ}	4	4881	3746	1.3
		χ	18	21456	3746	5.73
		$\log(\sigma)$	2	3834	3746	1.02

703

Table D.3: Fitting times for the Schaefer, Fox, Pella-Tomlinson and new model, in 3 separate runs. Bold font indicates the run used in the Results section. Run time for 10,000 iterations is presented in seconds, whilst 1,000,000 iterations is recorded in minutes. Difference is the time in minutes between the fastest and slowest run time.

Model	Run 1		Run 2		Run 3		
	10^4 its.	10^6 its.	10^4 its.	10^6 its.	10^4 its.	10^6 its.	Difference
Schaefer	31	48	30	48	**32**	**47**	1
Fox	61	55	**69**	**50**	35	59	9
Pella-Tomlinson	39	63	39	62	**36**	**60**	3
New model	14	28	14	24	**14**	**24**	4

Table F.1: True surplus production equation and values for hyperparameters used in two simulated data sets.

	Simulation 1	Simulation 2
True surplus equation	Schaefer (eq. 4)	New (eq. 10)
Parameters	$K = 1000$	$e^{\rho} = 1000$
	$q = 0.003$	$e^{\chi} = 0.003$
	$r = 0.2$	$\phi = 0.3$
	$\sigma = 0.0025$	$\sigma = 0.0025$

Table F.2: Simulated data sets under the conditions specified in Table F.1.

	Simul. 1			Simul. 2		
Year	Biomass	Catch	Effort	Biomass	Catch	Effort
1971	689	304	100	599	365	200
1972	487	221	100	351	194	200
1973	427	142	100	264	155	200
1974	347	138	100	208	131	200
1975	300	105	100	192	114	200
1976	239	101	100	158	102	200
1977	194	76	100	150	95	200
1978	168	56	100	142	84	200
1979	137	53	100	139	81	200
1980	119	43	100	136	92	200
1981	98	36	100	138	80	200
1982	79	30	100	141	89	200
1983	75	24	100	135	78	200
1984	69	24	100	126	72	200
1985	59	21	100	139	88	200
1986	65	5	25	137	88	200

	Simul. 1			Simul. 2		
Year	Biomass	Catch	Effort	Biomass	Catch	Effort
1987	70	5	25	133	83	200
1988	76	6	25	135	79	200
1989	74	6	25	148	64	150
1990	84	6	25	160	69	150
1991	97	7	25	170	72	150
1992	100	7	25	195	89	150
1993	99	7	25	187	88	150
1994	123	7	25	198	90	150
1995	134	9	25	205	92	150
1996	135	9	25	212	95	150
1997	145	11	25	200	87	150
1998	161	11	25	211	85	150
1999	170	13	25	225	99	150
2000	184	12	25	225	95	150

Table F.3: Percentage and absolute difference between true parameter values and posterior means, posterior means, standard deviations, coefficients of variation and percentiles for model parameters, under the four models (Schaefer, Fox, Pella-Tomlinson, New) for Simulated data set 1.

model	parameter	% diff.	abs. diff.	mean	st. dev.	c.v.	2.5%	median	97.5%
Sch.	r	-19%	0.038	0.162	0.021	0.13	0.121	0.162	0.203
	K	+8%	78	1078	85	0.08	927	1072	1263
	q	-7%	0.0002	0.0028	0.0002	0.08	0.0024	0.0028	0.0032
	σ	+14%	0.00036	0.0029	0.0008	0.3	0.0017	0.0027	0.0049
Fox	r	+103%	0.206	0.406	0.05	0.12	0.306	0.406	0.503
	K	+19%	190	1190	101	0.08	1012	1183	1411
	q	-16%	0.0005	0.0025	0.0002	0.08	0.0021	0.0025	0.0029
	σ	+22%	0.00055	0.0031	0.0009	0.3	0.0018	0.0029	0.0053
P.-T.	r	-91%	0.182	0.018	0.007	0.38	0.01	0.017	0.035
	K	+213%	2134	3134	3854	1.23	110	1269	13530
	q	+124%	0.0037	0.0067	0.0084	1.26	0.0002	0.0025	0.0294
	ϕ	NA	NA	0.0336	0.0559	1.66	0.0008	0.0105	0.18
	σ	323%	0.00808	0.0106	0.0033	0.31	0.006	0.01	0.0187

model	parameter	% diff.	abs. diff.	mean	st. dev.	c.v.	2.5%	median	97.5%
New	ϕ	NA	NA	0.06	0.008	0.13	0.044	0.06	0.076
	e^{ρ}	+9%	87	1087	108	0.1	897	1080	1326
	e^{χ}	-9%	0.0003	0.0027	0.0002	0.08	0.0023	0.0027	0.0032
	σ	+39%	0.00097	0.0035	0.001	0.29	0.002	0.0033	0.0059

Table F.4: Fitting times for the Schaefer, Fox, Pella-Tomlinson and New model, in 3 separate runs for Simulation 1. Bold font indicates the run used for results. Run time for 10,000 iterations is presented in seconds, whilst 1,000,000 iterations is recorded in minutes. Difference is the time in minutes between the fastest and slowest run time.

Model	Run 1		Run 2		Run 3		
	10^4 its.	10^6 its.	10^4 its.	10^6 its.	10^4 its.	10^6 its.	Difference
Schaefer	31	48	30	48	**32**	**47**	1
Fox	61	55	**69**	**50**	35	59	9
Pella-Tomlinson	39	63	39	62	**36**	**60**	3
New model	14	28	14	24	**14**	**24**	4

Table F.5: Percentage and absolute difference between true parameter values and posterior means, posterior means, standard deviations, coefficients of variation and percentiles for model parameters, under the four models (Schaefer, Fox, Pella-Tomlinson and new) for Simulated data set 2.

model	parameter	% diff.	abs. diff.	mean	st. dev.	c.v.	2.5%	median	97.5%
Sch.	r	NA	NA	0.63	0.395	0.63	0.07	0.572	1.956
	K	+166%	1661	2661	3180	1.2	706	806	11910
	q	+820%	0.0026	0.0276	0.04	1.45	0.0019	0.0024	0.1253
	σ	+8392%	0.20980	0.2123	0.3158	1.49	0.0012	0.0023	0.9144
Fox	r	NA	NA	2.031	0.121	0.06	1.786	2.033	2.26
	K	-17%	170	830	49	0.06	744	826	938
	q	-26%	0.0026	0.0022	0.0002	0.08	0.0019	0.0022	0.0026
	σ	-28%	0.00069	0.0018	0.0005	0.3	0.0011	0.0017	0.0031
P.-T.	r	NA	NA	0.103	0.025	0.24	0.068	0.097	0.164
	K	+145%	1454	2454	3441	1.4	119	754	12700
	q	+59%	0.0026	0.0048	0.0051	1.06	0.0001	0.0024	0.0162
	ϕ	-21%	0.0634	0.2366	0.2821	1.19	0.0052	0.0929	0.9318
	σ	+42%	0.00105	0.0036	0.0011	0.3	0.002	0.0034	0.0061

model	parameter	% diff.	abs. diff.	mean	st. dev.	c.v.	2.5%	median	97.5%
New	ϕ	+21%	0.062	0.362	0.032	0.09	0.299	0.362	0.426
	e^{ρ}	-31%	309	691	59	0.09	587	686	821
	e^{χ}	-12%	0.0004	0.0026	0.0003	0.1	0.0021	0.0026	0.0032
	σ	-3%	0.00007	0.0024	0.0007	0.3	0.0014	0.0023	0.0042

Table F.6: Fitting times for the Schaefer, Fox, Pella-Tomlinson and new model, in 3 separate runs for Simulation 2. Bold font indicates the run used for results. Run time for 10,000 iterations is presented in seconds, whilst 1,000,000 iterations is recorded in minutes. Difference is the time in minutes between the fastest and slowest run time.

Model	Run 1		Run 2		Run 3		
	10^4 its.	10^6 its.	10^4 its.	10^6 its.	10^4 its.	10^6 its.	Difference
Schaefer	39	67	**37**	**59**	40	69	10
Fox	55	78	**46**	**76**	61	77	2
Pella-Tomlinson	**55**	**84**	51	87	51	85	3
New model	20	33	20	33	**20**	**33**	0

H List of appendix figures

Figure A.1: Novel production function for various elasticities (ϕ) and biomass depletion ratios (B/K).

Figure A.2: Logistic production function (Verhulst, 1838; Schaefer, 1954) for various intrinsic growth rates (r) and biomass depletion ratios (B/K)

Figure A.3: Gompertz production function (Fox, 1970), for various instantaneous growth rates (r) and biomass depletion ratios (B/K).

Figure A.4: Production function of Pella and Tomlinson (1969), for a set elasticity (ϕ) and various instantaneous growth rates (r) and biomass depletion ratios (B/K).

Figure D.1: Schaefer model posterior probability distributions of parameters r, K and q and MSY on the diagonal, correlations above the diagonal and scatter plots with LOWESS curves below the diagonal.

Figure D.2: Fox model posterior probability distributions of parameters r, K and q and MSY on the diagonal, correlations above the diagonal and scatter plots with LOWESS curves below the diagonal.

Figure D.3: Pella-Tomlinson model posterior probability distributions of parameters r, K, q and ϕ and MSY on the diagonal, correlations above the diagonal and scatter plots with LOWESS curves below the diagonal.

Figure D.4: The new model's posterior probability distributions of parameters ϕ, e^{ρ} and e^{χ} and MSY on the diagonal, correlations above the diagonal and scatter plots with LOWESS curves below the diagonal.

Figure D.5: MSY posterior densities for the new model (solid black line), Schaefer (dashed red line), Fox(dotted green line) and Pella-Tomlinson (dashed and dotted blue line).

Figure E.1: Plots of the Namibian hake fishery, provided by the Shiny app in the `R`

728 package `rcsurplus`.

729 Figure E.2: Specification of model priors and MCMC parameters, in the Shiny app in

730 the `R` package `rcsurplus`.

731 Figure E.3: A plot of model fits, provided by the Shiny app in the `R` package `rcsurplus`.

I Appendix figures

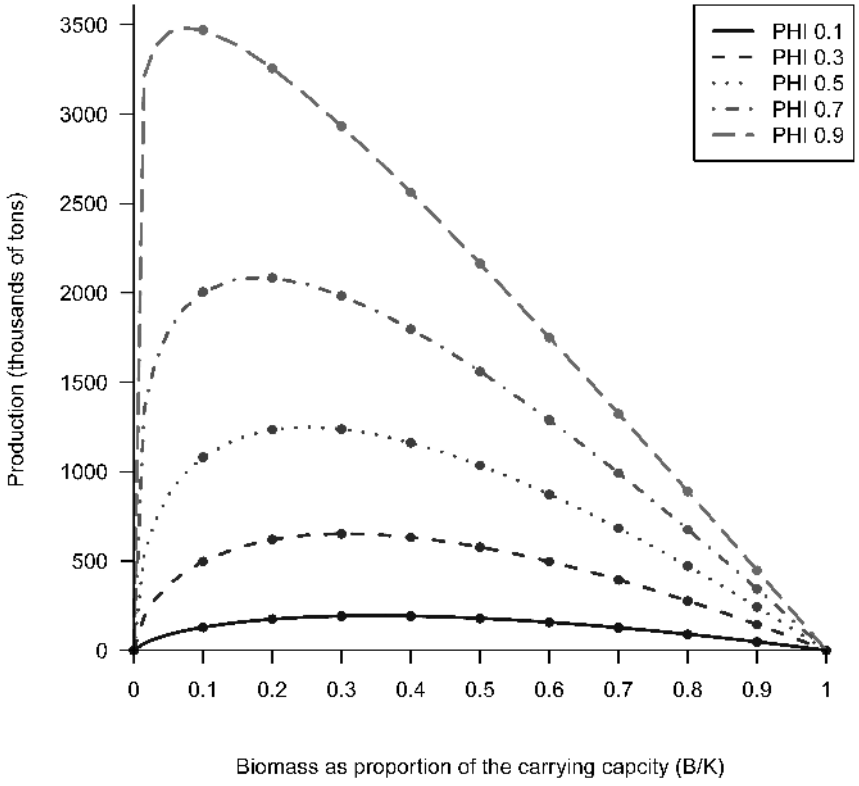

Figure A.1: Novel production function for various elasticities (ϕ) and biomass depletion ratios (B/K).

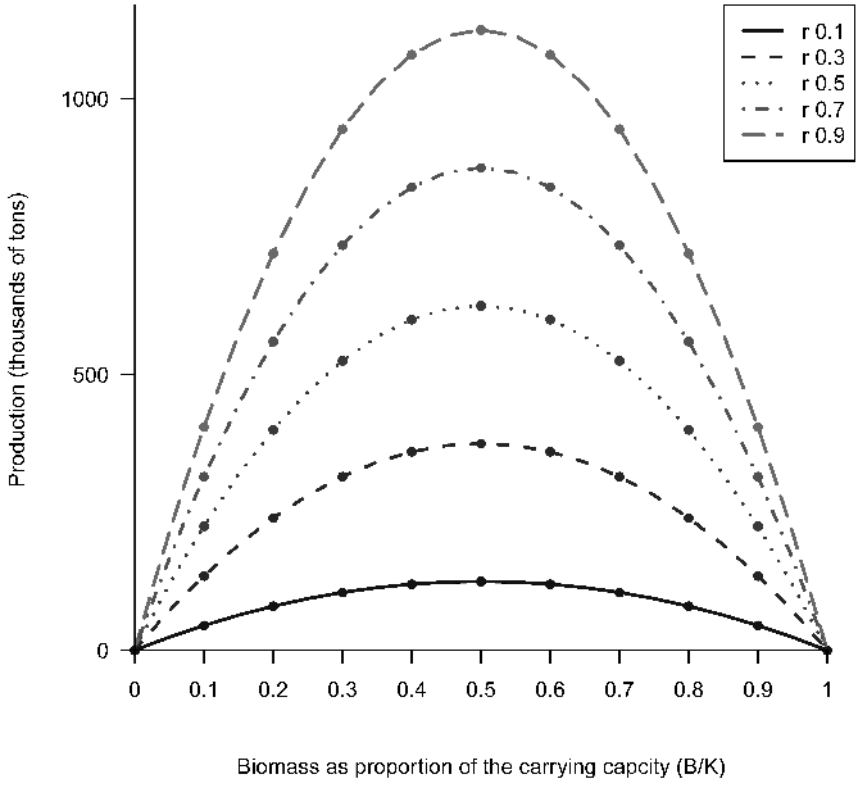

Figure A.2: Logistic production function (Verhulst, 1838; Schaefer, 1954) for various intrinsic growth rates (r) and biomass depletion ratios (B/K).

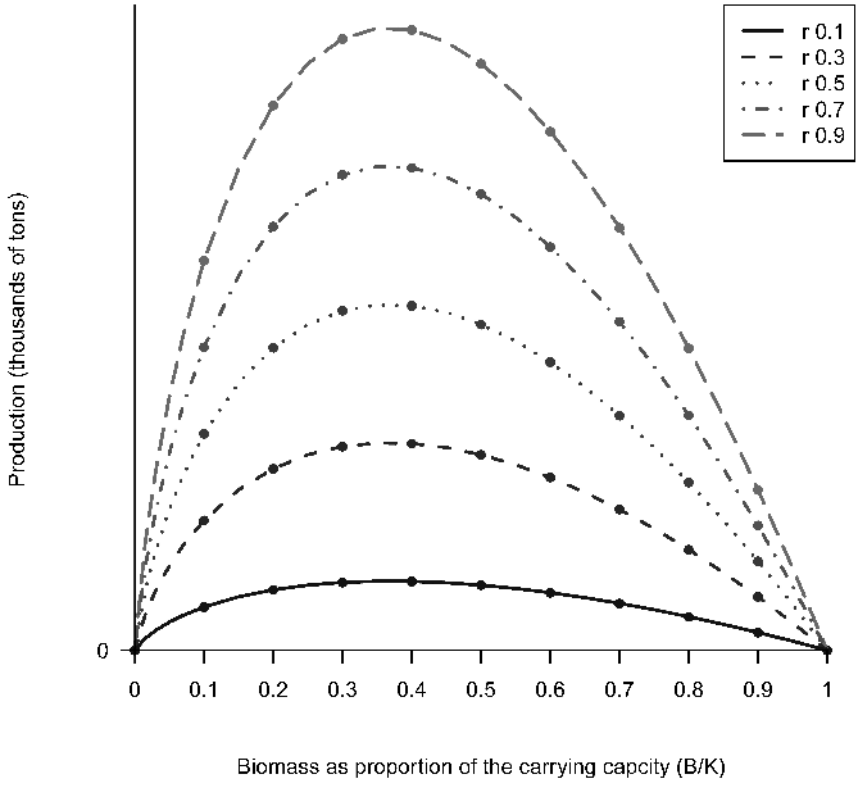

Figure A.3: Gompertz production function (Fox, 1970), for various instantaneous growth rates (r) and biomass depletion ratios (B/K).

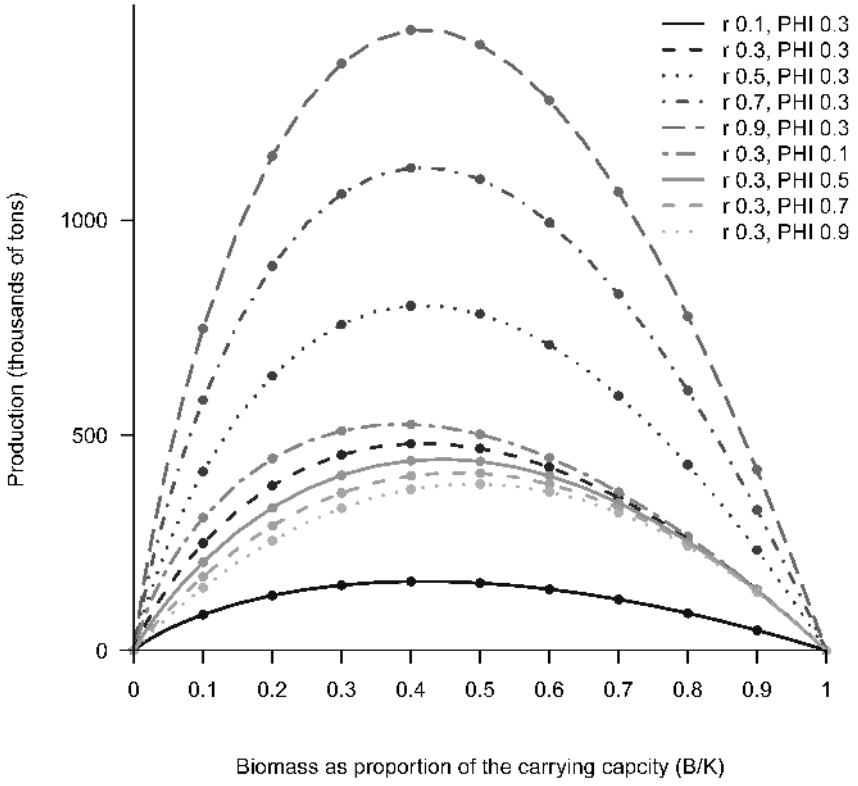

Figure A.4: Production function of Pella and Tomlinson (1969), for various elasticity (ϕ) and instantaneous growth rates (r) and biomass depletion ratios (B/K).

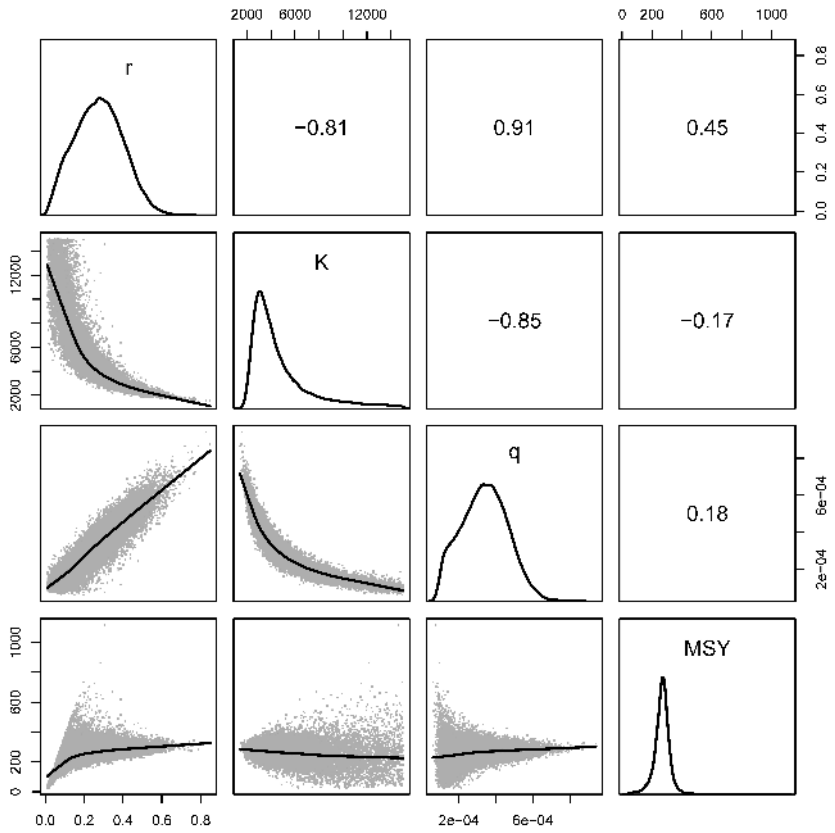

Figure D.1: Schaefer model posterior probability distributions of parameters r, K and q and MSY on the diagonal, correlations above the diagonal and scatter plots with LOWESS curves below the diagonal.

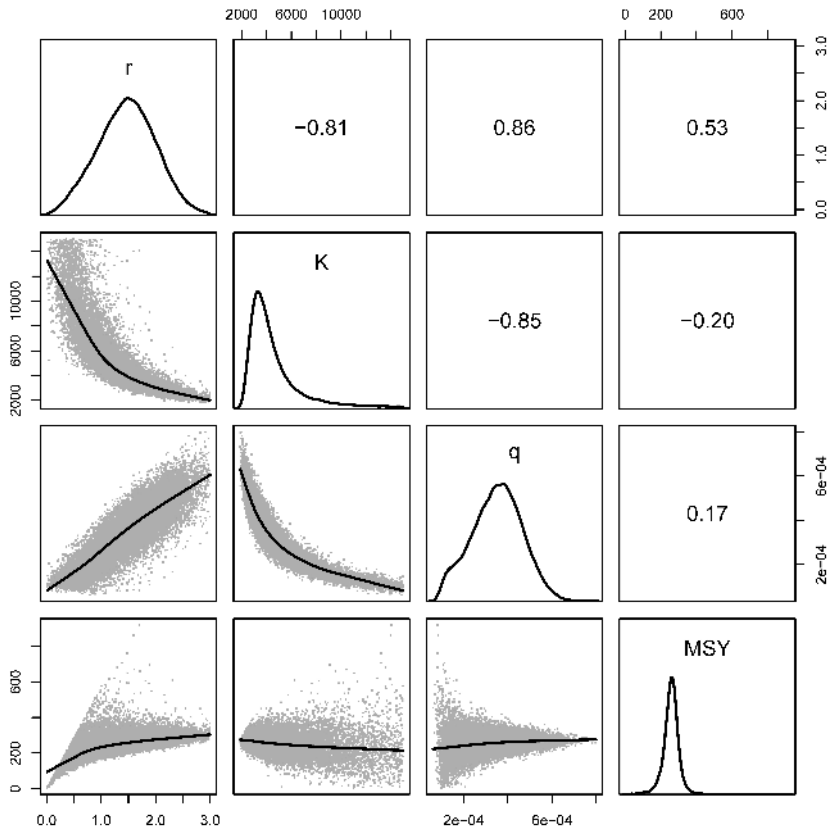

Figure D.2: Fox model posterior probability distributions of parameters r, K and q and MSY on the diagonal, correlations above the diagonal and scatter plots with LOWESS curves below the diagonal

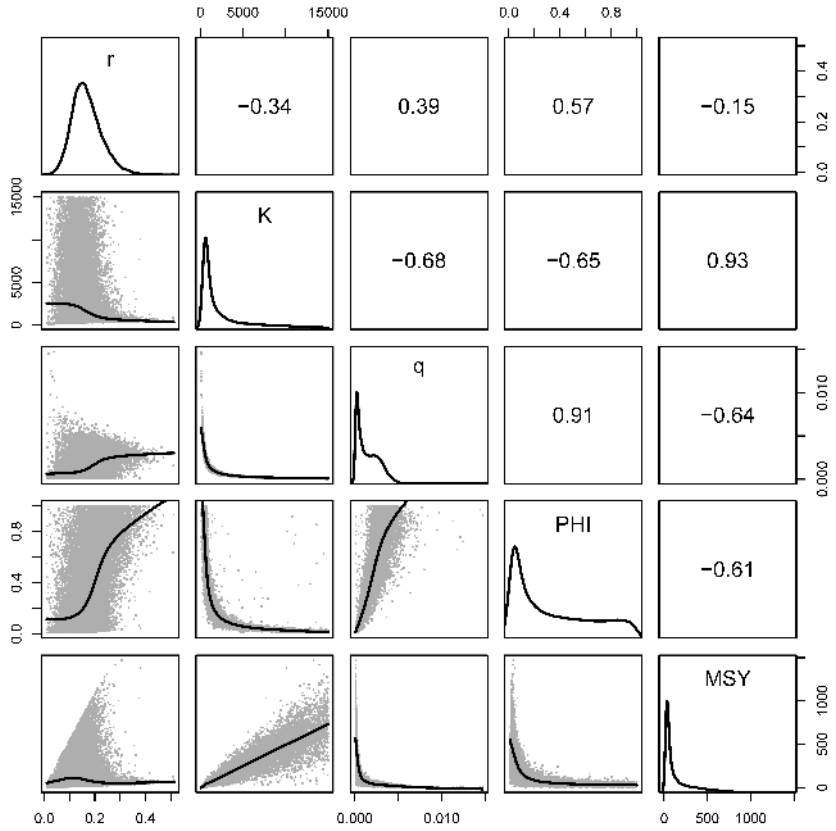

Figure D.3: Pella-Tomlinson model posterior probability distributions of parameters r, K, q and ϕ and MSY on the diagonal, correlations above the diagonal and scatter plots with LOWESS curves below the diagonal.

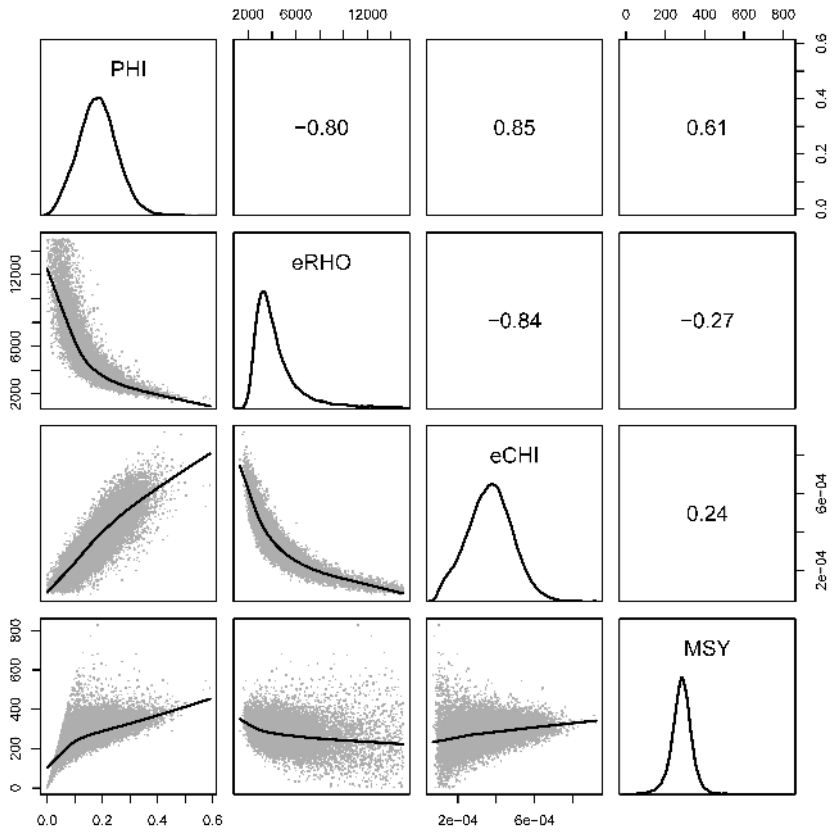

Figure D.4: The new model's posterior probability distributions of parameters ϕ, e^{ρ} and e^{χ} and MSY on the diagonal, correlations above the diagonal and scatter plots with LOWESS curves below the diagonal.

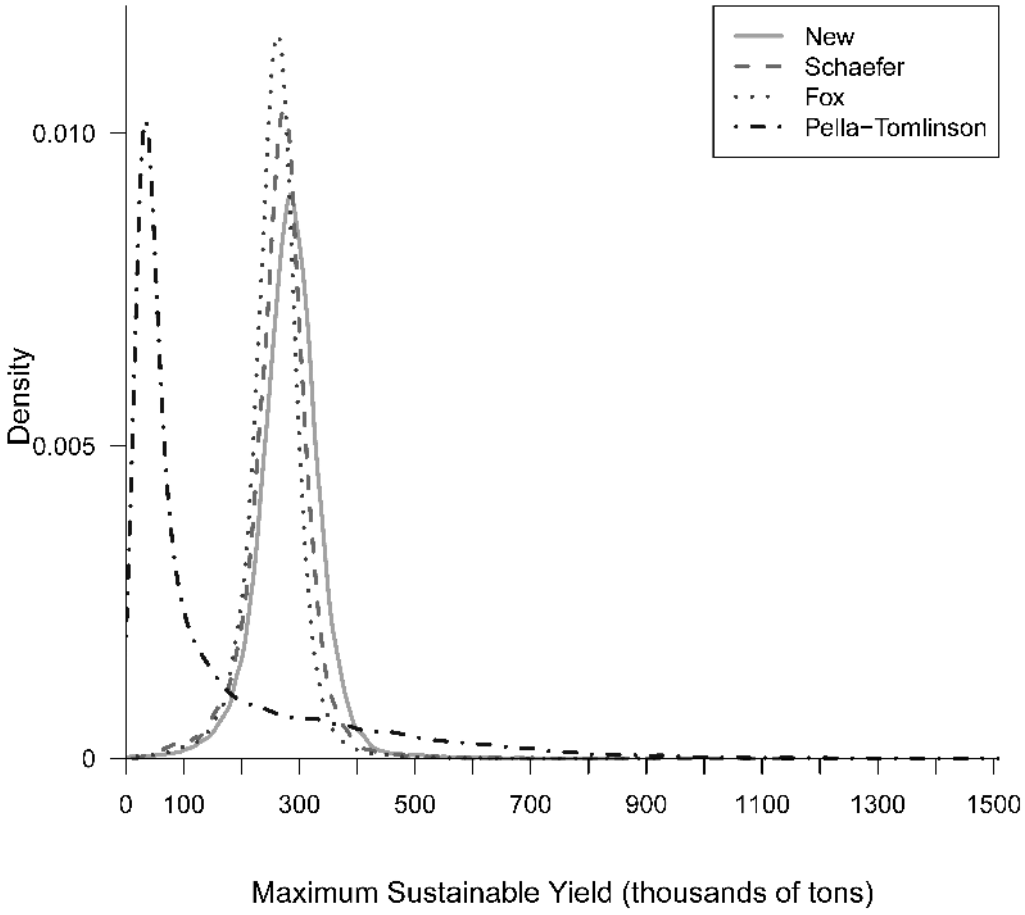

Figure D.5: MSY posterior densities for the new model (solid black line), Schaefer (dashed red line), Fox(dotted green line) and Pella-Tomlinson (dashed and dotted blue line).

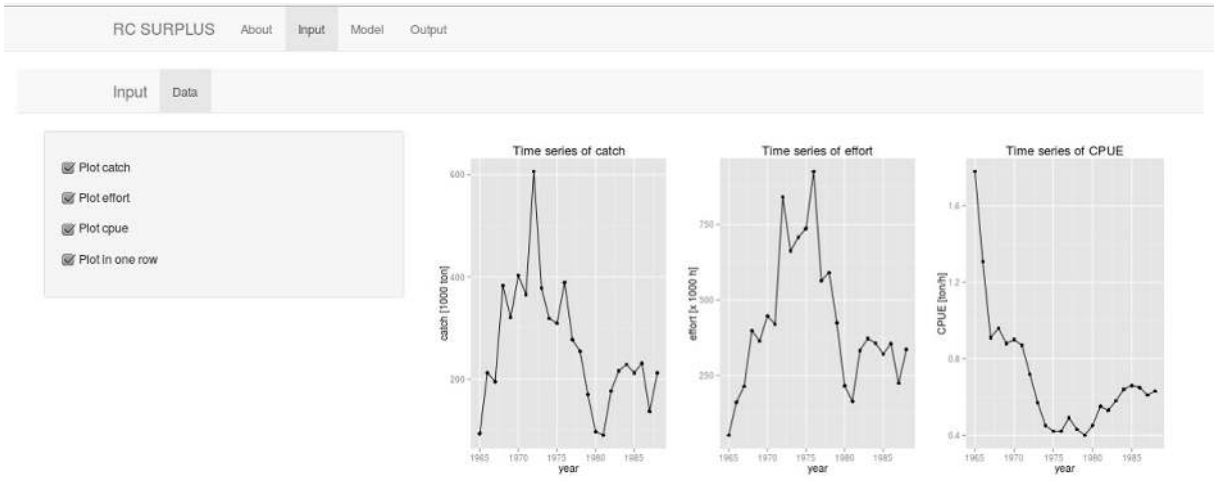

Figure E.1: Plots of the Namibian hake fishery, provided by the Shiny app in the `R` package `rcsurplus`.

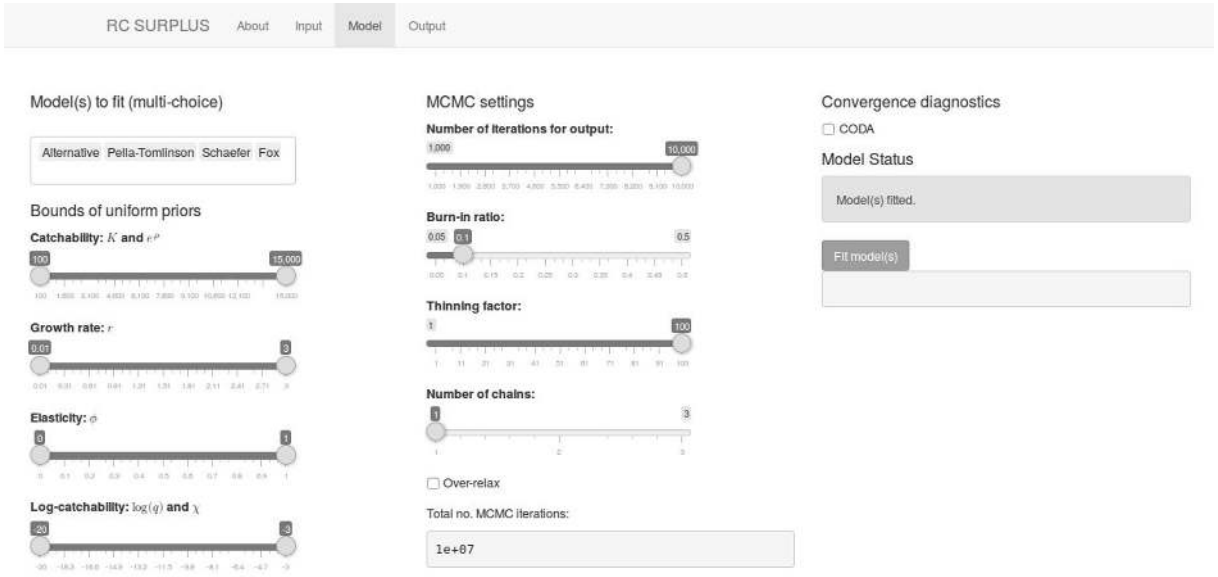

Figure E.2: Specification of model priors and MCMC parameters, in the Shiny app of the `R` package `rcsurplus`.

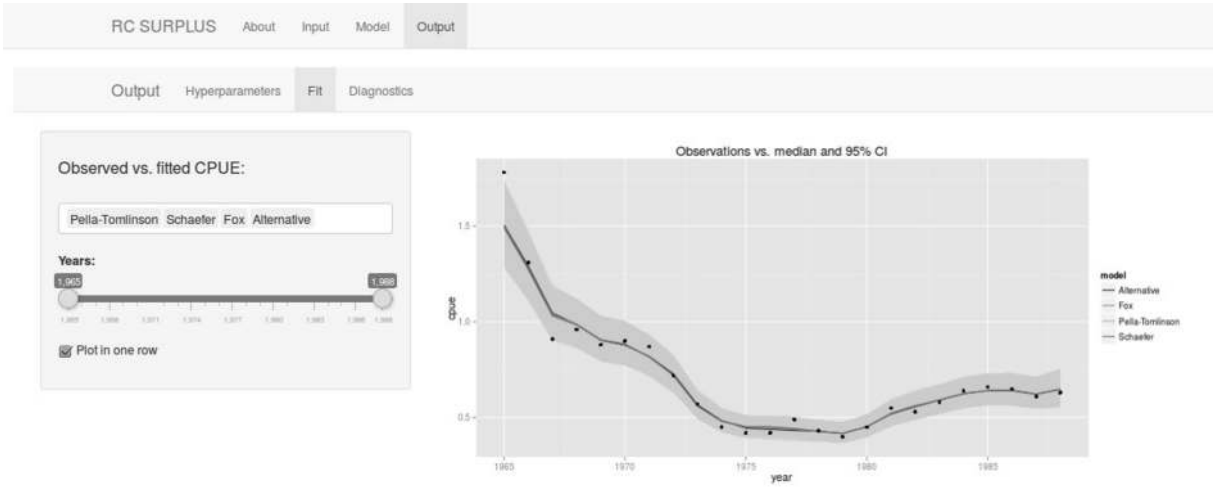

Figure E.3: A plot of model fits, provided by the Shiny app in the `R` package `rcsurplus`.